SAI/1999-083/Rp

2nd POST-OPERATIONS CROSS-CALIBRATION STATUS REPORT

v1.0

December 2, 1999

P. García-Lario

1 Introduction

1.1 Scope

1.2 Structure of cross-calibration activities

1.3 Final Goals: General

1.4 Final Goals: per Working Group

1.4.1 Aperture/Beam Profiles, PSFs and Straylight

1.4.2 Glitch Effects

1.4.3 Line profiles

1.4.4 Photometric calibration

1.4.5 Polarisation

1.4.6 Spectral Matching and RSRF

1.4.7 Transients

1.4.8 Interactive Analysis

2 Review of Cross-Calibration Plan

2.1 Overview of Working Group activities

2.2 Report on actions on-going and/or closed

2.3 Updated overall schedule

3 Internal and external cross-calibration

3.1 The concept of cross-calibration

3.2 Definition of standard and cross-calibration sources

3.3 A new cross-calibration strategy

3.4 Cross-calibration comparisons

4 Calibration accuracies and 'Error Budget'

4.1 PHT

4.1.1 Improvements in OLPv8.4 for PHT

4.1.2 Current calibration accuracies and 'Error Budget' for PHT

4.1.3 Future plans in PHT calibration

4.2 SWS

4.2.1 Improvements in OLPv8.4 for SWS

4.2.2 Current calibration accuracies and 'Error Budget' for SWS

4.2.3 Future plans in SWS calibration

4.3 CAM

4.3.1 Improvements in OLPv8.0 for CAM

4.3.2 Current calibration accuracies and 'Error Budget' for CAM

4.3.3 Future plans in CAM calibration

4.4 LWS

4.4.1 Improvements in OLPv8.7 for LWS

4.4.2 Current calibration accuracies and 'Error Budget' for LWS

4.4.3 Future plans in LWS calibration

1 Introduction

1.1 Scope

This is the second of a series of Reports generated every six months by the ISO Data Centre (IDC, hereafter) which tries to summarize the up-to-date status of (cross-)calibration activities during the ISO Post-Operations (POPS, hereafter) Phase as of November 1999.

It includes information on the latest achievements in the calibration of all four ISO instruments with special emphasis on cross-calibration aspects as well as an assessment of the progress made in the last six months within the framework of the POPS Cross-calibration Plan.

The previous (first) Status Report can be found at:

`\http://www.iso.vilspa.esa.es/users/expl_lib/ISO/1st_status_report_ext.ps.gz`

This series of Status Reports will culminate in the final POPS Cross-calibration Status Report at the end of the Post-Operations phase to be issued in April 2001.

1.2 Structure of cross-calibration activities

The global IDC strategy for approaching cross-calibration during the Post-Operations phase, as previously described in the ISO POPS Cross-Calibration Plan, is based on topic-oriented Working Groups, each one of them addressing one specific calibration topic.

Working Groups are formed by members from the IDC and from the different NDCs. They are also open to contributions from external individuals interested in actively participating in ISO calibration activities.

Currently, eight Working Groups (WG, hereafter) have been created and are actively working on:

- Beam Profiles/Pointing
- Glitch Effects
- Line profiles
- Photometric calibration
- Polarisation
- Spectral Matching and RSRF
- Transients
- Interactive Analysis

Note that the Interactive Analysis WG was activated only very recently and, thus, it was not yet included as a WG in the previous Status Report.

Of course, the topics addressed by each of these WGs overlap in many cases since many cuts through the calibration issue are possible. For example, studies of *Transients* are fundamental to a full understanding of the instruments' photometric calibration, which is the main goal of the *Photometric Calibration* WG. The WG scheme provides them with a platform to exchange their knowledge and to progress with respect to their own subject.

It is the responsibility of cross-calibration to maintain an overview of the work of the several Working Groups, cooperate with instrument-specific calibration manpower in efforts to understand inconsistencies of calibration relevant to more than one instrument and establish links between the different Working Groups when necessary favouring a fluid exchange of useful information.

An updated overview of the composition of each of these WGs can be found at:

`http://isowww.vilspa.esa.es/users/expl_lib/ISO/WG_COMPOSITION_2.PS`

1.3 Final Goals: General

The objectives of cross-calibration can be summarized as follows:

- Compare the results of different ISO instruments and verify the errors quoted for each instrument-specific calibration. Where these results appear to be inconsistent seek to understand and to eliminate those differences.
- Compare ISO results with external data (e.g. ground based observations, KAO data, IRAS, COBE, ...). Where results appear to be inconsistent seek to understand and to eliminate those differences.
- Verify that, from a more global point of view, the calibrations of the individual ISO instruments are correct, and ensure a certain level of homogeneity and consistency of the data and how they were calibrated (e.g. compatibility of models, bandpass zero-points, and of calibration philosophy and procedures).

The intention is to have a flexible plan/strategy with these goals as a reference which is materialized in a detailed schedule of cross-calibration activities for each of the Working Groups listed above.

Responsibility for cross-calibration planning is with the IDC in close interaction with the NDCs which are responsible for instrument-specific calibration.

1.4 Final Goals: per Working Group

1.4.1 Beam Profiles/Pointing

· Characterization of the instruments' beam profiles.

· Address common problems (asymmetries, vignetting, ghosts,..) and their possible relation to the ISO telescope point spread function (PSF).

· Allow cross-fertilisation of models available.

· Evaluation of common deconvolution tools, to apply to extended source data, once beam profile calibration files become available.

· Support improvement of ISO pointing reconstruction in OLP.

1.4.2 Glitch Effects

· Statistical analysisis and characterization of glitches in the four ISO instruments. Study of the relation with the space radiation environment.

· Compare glitch statistics and glitch height distributions with model predictions and simulations.

· Enhance the quality of the reduced ISO data, improving the de-glitching and de-tailing algorithms in the pipeline and/or IA.

· Keep the knowledge on the radiation environment and its effects on the detectors, so that it can be applied to future missions, in particular FIRST.

1.4.3 Line profiles

· Characterize the SWS and LWS observed instrumental profiles.

· Study the stability of these instrumental profiles as a function of time, forward and backward scans, detector, line strength and point-like versus extended sources.

· Analysis and interpretation of deviations found from line profile definition; recommendations and caveats.

· Comparison with theoretical instrumental profiles and resolution.

1.4.4 Photometric calibration

· Definition of the photometric system and description of calibration sources/models used in ISO data reduction.

· Characterization of the photometric accuracies achieved by each ISO AOT (and the corresponding photometric 'error budget').

· Make periodic 4-instrument photometric comparisons on selected sample targets and extend this comparison to calibration models and to photometric results obtained with other facilities (DIRBE/IRAS/KAO, ground-based,..) using OLP data products.

· Make similar comparisons on a subsample of targets using data reduced with the latest available versions of the instrument IAs and compare this with OLP photometric accuracies.

· Testing of photometric improvements as new algorithms or calibration files become available stimulating their inclusion into the corresponding IAs first and eventually into the pipeline.

· Identification and analysis of photometric calibration problems affecting OLP data products providing recommendations and caveats to the users of the ISO Legacy Archive.

1.4.5 Polarisation

· Characterization of the polarimetric capabilities of ISO. Angles, detection limits, wavelength dependency, internal consistency (PHT,CAM) and comparison with external data.

1.4.6 Spectral Matching and RSRF

· Analysis of spectral matching between LWS and SWS in the overlapping region. Same with CAM-CVF and PHT-S spectra. Comparison with models.

· Identification of possible systematic errors in the measured spectral response to extended sources by comparing the observations from a variety of instruments. Effects on the determination of spectral line fluxes.

· Expansion of cross-calibration between the instruments beyond the wavelength regions which they have in common.

· Characterization of the Relative Spectral Response Function (RSRF) for all ISO spectroscopic modes.

1.4.7 Transients

· Characterize transient effects in the 4 ISO instruments and determine the best correction method as a function of detector type, observing mode and characteristics of the source, and estimation of effects on photometric accuracy.

· Stimulate the development of S/W tools to detect and correct transient effects in IA first and eventually the implementation of these tools in OLP.

1.4.8 Interactive Analysis

· Coordinate the information flow between developers of the different instruments' IAs. Each team should be aware of what other teams are doing. S/W tools developed by one of the teams should be made available to other teams if they consider it useful.

· Stimulate the implementation of new S/W tools in the four ISO instruments' IAs.

· Raise the profile of the various IA packages as means to enhance data reduction.

· Investigate communication channels between the IA users and IA developers in both directions.

2 Review of Cross-Calibration Plan

2.1 Overview of Working Group activities

As it was defined in the ISO POPS Cross-Calibration Plan, the WGs should:

- look at major calibration issues across instrument boundaries
- identify problems, (interim-)goals and milestones (usually linked to OLP milestones)
- trigger/recommend further work, and recognise imperatives in their area
- establish and pursue relevant contacts in NDCs
- identify good calibration sources and strategies.

In order to achieve these goals each WG was requested to define a list of actions, goals and milestones with an associated schedule which was used as initial basis for the elaboration of the Cross-Calibration Plan.

2.2 Report on actions on-going and/or closed

A number of actions included in the Cross-Calibration Plan, as it was proposed in the previous Status Report, have been closed in the last six months. In the following, a summary of the main results found and conclusions reached is provided sorted by WG. In some cases, the activities described below were not directly carried out by members of the WG but they have been included because they might be relevant for the future planning of the WG or to illustrate a progress on the current understanding of a problem under analysis by a specific WG.

Beam Profiles/Pointing :

`BP: ISO telescope asymmetric PSF model revision (September 1999)`
`Koryo Okumura`

In a previous WG meeting Koryo Okumura suggested that a displacement in the secondary mirror of ISO of 0.3 mm perpendicular to the optical axis could explain the asymmetric PSF observed (see Figure 1).

This result was derived using the ASAP simulation software and it has been found to be in agreement with FFT-based calculations made assuming a phase shift (see Figure 2).

FFT-based models are easier to compare with the observed PSF and they reproduce also the observed trend for the asymmetry, getting stronger at shorter wavelengths, confirming the results previously obtained with ASAP.

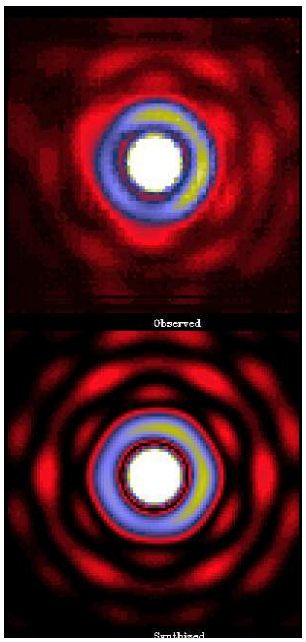

Figure 1: Observed (top) and synthesized with ASAP (bottom) PSFs: 1.5 arcsec PFOV at LW9 (15 μm) - Koryo Okumura

Other alignment offsets have also been considered with ASAP. It was found that a further, small displacement along the optical axis can explain the observed dip in the azimuthal profile of the PSF first Airy ring. The two offsets are complementary. However, no parameter set has yet been defined, able to accurately reproduce the overall observed assymetry.

Unfortunately, it is not possible to compare the above results with any tolerance value or any other data measured during the optical alignment of ISO since it seems that the telescope was aligned just by maximizing the image quality and the position of the secondary mirror was never measured.

Taking the above results into account, other ISO instruments are invited to check whether their beam profiles also show a similar asymmetry and/or to use the ISO PSF model derived from CAM observations as input for their beam profile models. Note that in some cases the sensitivity of other instruments like PHT might not be enough to detect any fine structure in the first Airy ring and, thus, the comparison might not be possible.

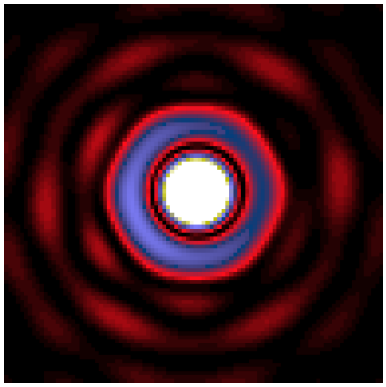

Figure 2: PSF computed with a phase shift using FFT-based calculations. Note that it shows an asymmetry very similar to that obtained with ASAP simulations - Koryo Okumura

`BP: SWS Beam profile model (June 1999)`
`Douwe Beintema`

Douwe Beintema modelled the SWS beam profile, fine tuned to fit merged data sets of calibration observations consisting of rasters made on several point sources. Model and observations are compared for the different SWS bands in Figure 3 (y-axis) and 4 (z-axis) with a general good agreement.

The main problem found is that the beams are in many cases not flat-topped. This makes SWS very sensitive to small pointing offsets. In addition, there are strong internal detector misalignments which can reach up to $8''$ and produce mismatches between different bands.

`BP: SWS Beam profile calibration files (July 1999)`
`Rosario Lorente + Alberto Salama`

The SWS beam profile model provided by Douwe Beintema was used as input for the production of the corresponding calibration files. They were generated by covering an area of $6' \times 6'$ with a spacing of $1''$. These new Cal-G files are expected to be of extraordinary help in the calibration of extended sources and bad-pointed observations. They will be implemented in the next version of

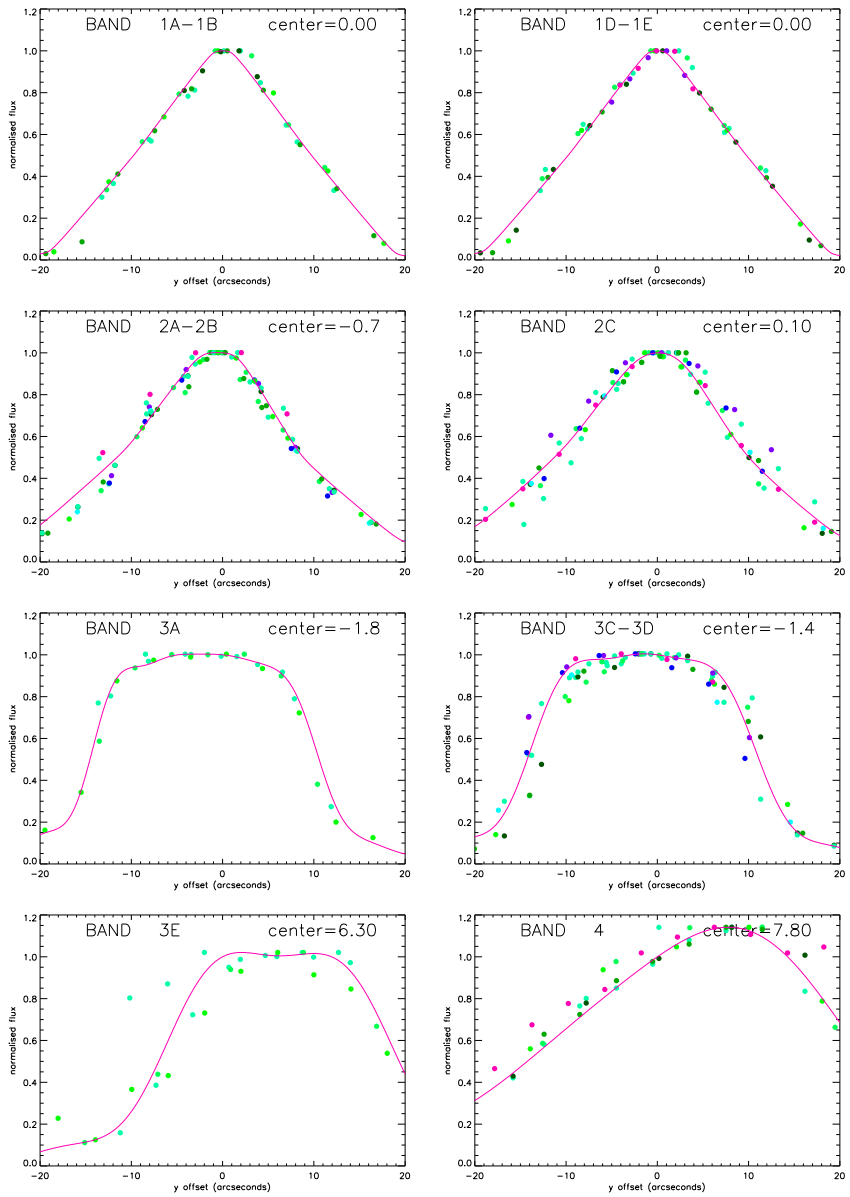

Figure 3: SWS beam profiles. Comparison between model and observations in the y-axis for the different SWS bands - Douwe Beintema

the SWS IA but, unfortunately, they will have to wait for version 9.5 to be implemented in the SWS pipeline (September 2000).

`BP: Characterization of the LWS Beam profile: conversion factors from point source to extended source fluxes available in ISAP 2.0 (July 1999)`
`Chris Lloyd`

Chris Lloyd derived conversion factors from point source to extended source fluxes from the LWS mean beam profile (averaged over radial directions) based just on the core of the beam profile. These factors as well as IDL routines to compute the mean beam as a function of position will be part of the final version

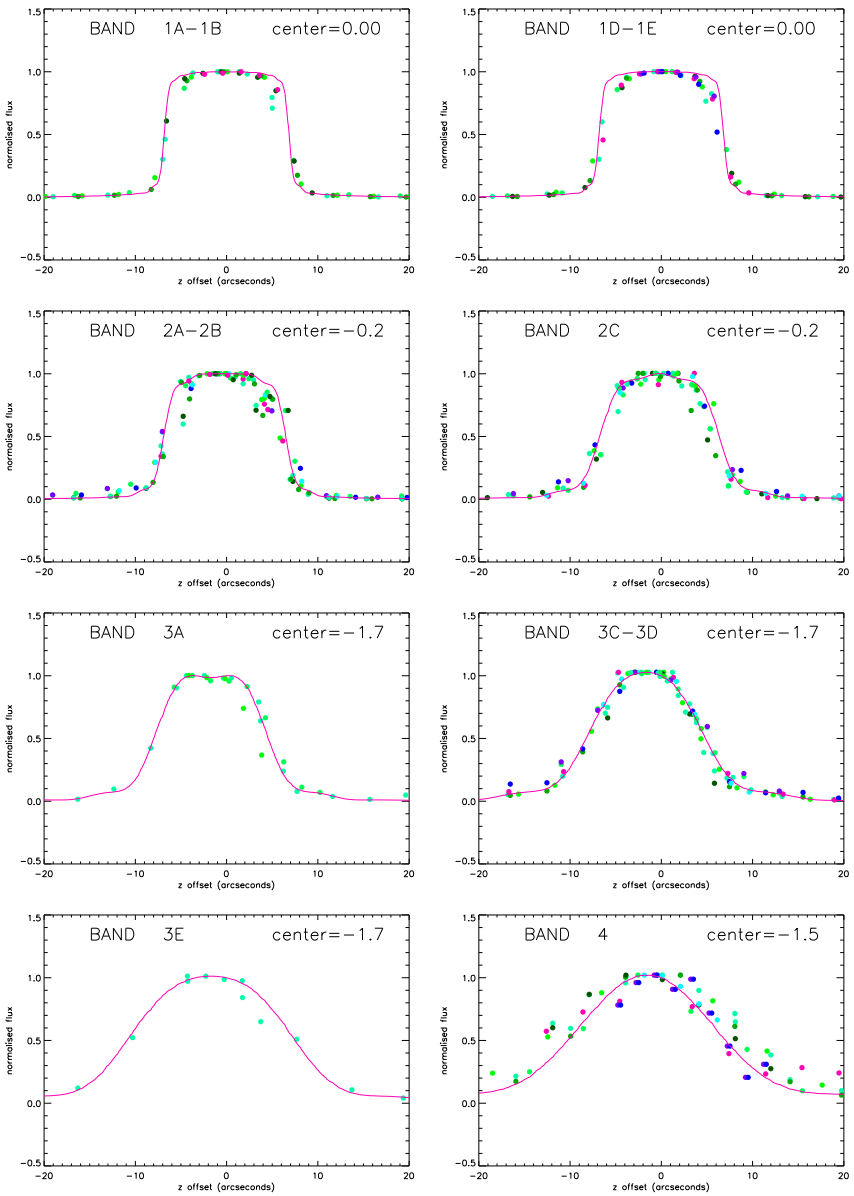

Figure 4: SWS beam profiles. Comparison between model and observations in the z-axis for the different SWS bands - Douwe Beintema

of ISAP 2.0 (release expected December 15, 1999)

Application of these conversion factors to a few LWS rasters scans on extended sources by Martin Burgdorf indicates that they significantly improve the level of agreement of ISO calibration with the flux derived from IRAS maps of the same positions in the sky at 100 μm (up to the 10% level).

`BP: PHT C100, C200 point spread function fractions available in PIA (August 1999)`
`Rene Laureijs`

The document *Point Spread Functions related to the ISOPHOT C100 and C200 arrays* by Rene Laureijs can be found at:

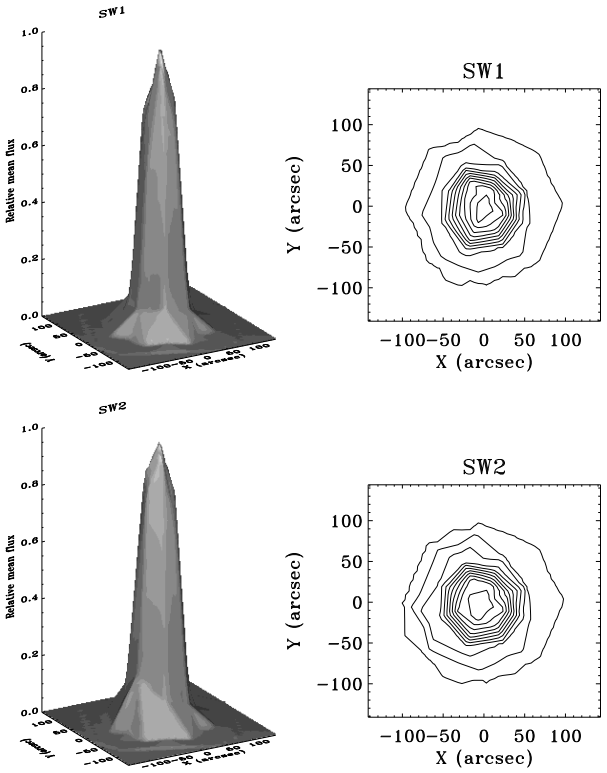

Figure 5: 3-D and contour plots of the beam profile of the LWS detectors SW1 and SW2 - Chris Lloyd

`http://www.iso.vilspa.esa.es/users/expl_lib/PHT/c200fpsf02.ps.gz`

The fraction of the PSF falling on individual C100 or C200 pixels has been determined per filter for a number of typical pointing configurations. The measurements were made on asteroids, outer planets (Uranus and Neptune) and bright stars such as α Boo (HR 5340). Comparison between the measured values and model computations show significant discrepancies for some of the C200 filters.

The values of the fractional PSF so calculated can be used to improve the point source photometry in minimaps and in source-background pointings, and to decide whether a source is extended.

Theoretical footprint files are available for P2, P3, C100 and C200 in Cal-G files v5.4.

BP: New ISO Pointing reconstruction Cal-G files containing Tycho data for guide stars implemented in OLP (November 1999)
Andy Pollock

The new ISO Pointing Reconstruction now considers the effects of differential aberration, proper motion and parallax of guide stars used for pointing.

While aberration was thought to be corrected for ISO observations by the fact that guidestars are always close ($\leq$ 2.5 degrees) to the observed target, the differential aberration effect can cause pointing errors up to 0.9" (if ISO's velocity is considered as well, this can become even larger).

On top of aberration two other significant sources of residual pointing errors were addressed, parallax and proper motion of guidestars. The effects are smaller ($\leq 0.4''$) but still significant in some cases, fortunately only affecting few nearby guidestars.

New Cal-G files were generated which correct for the Pointing Correction effects above refered and they have already been implemented in OLPv8.6.b1.

BP: SWS Pointing Correction Tool (July 1999)
Rosario Lorente + Alberto Salama

Calibration files for pointing correction and SSO tracking corrections were also generated considering the SWS beam profile model provided by Douwe Beintema. They consider absolute pointing offsets up to $30''$ with a resolution of $0.1''$ and are currently under testing.

BP: Workshop: "ISO Beyond point sources: studies of extended infrared emission" held at VILSPA (September 1999)

The aim of the meeting was to bring together scientists working on ISO programmes in which the analysis of extended emission is important, to exchange results and experiences.

The analysis of extended sources requires expertise in surface brightness calibration, map construction, and source flux extraction to arrive at reliable results and interpretation.

More than 40 astronomers attended the Workshop held at VILSPA from September 14 to 17, 1999. The final programme and abstracts of the presentations can be found at:

http://www.iso.vilspa.esa.es/meetings/isobeyond/fourth_announcement.html

The Proceedings of this Workshop will be published in the ESA Special Publications Series.

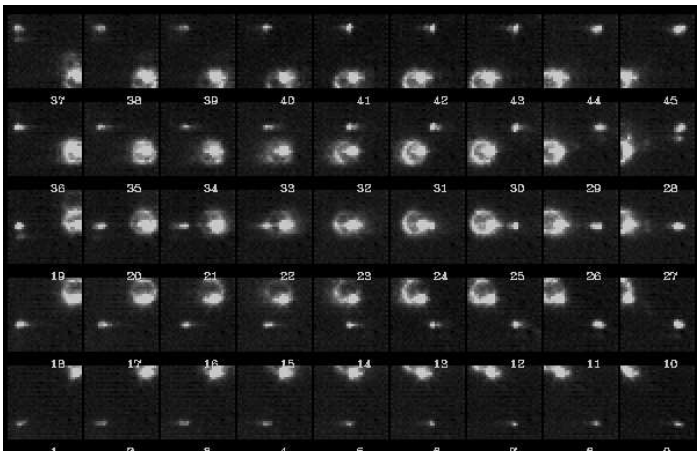

Figure 6: Global behaviour of ghosts when a point source moves over the detector (CVF at 7 μm with PFOV of 6$''$ in revolution 531) - Koryo Okumura

`BP: Analysis of ghosts in CAM images (July 1999) - Koryo Okumura`

Concerning ghost modelling, a considerable progress has been achieved by Koryo Okumura in the last six months. Ghost images are known to be a big problem for CAM since they strongly affect the photometry (up to 35% of the flux can be contained in the ghost in some cases). For point sources, always a primary ghost is located around the point source while a secondary point-like ghost is found near the symmetrical point with respect to the detector centre.

Using geometrical optics it is possible to determine the location of these multi-reflected images and the approximate size of the ghosts.

However, the brightness distribution of extended sources is affected by ray tracing noise, and a long computation time is needed to obtain some percent level structure. The results can strongly be improved by using the ASAP coherent light simulation software. With this tool it is possible to reproduce the brightness distribution and a more realistic size of the ghosts produced by point sources. In addition, the computation time may be shorter. However, it is not simple to make an ASAP code which works for any instrument configuration and for any location of the point source on the detector.

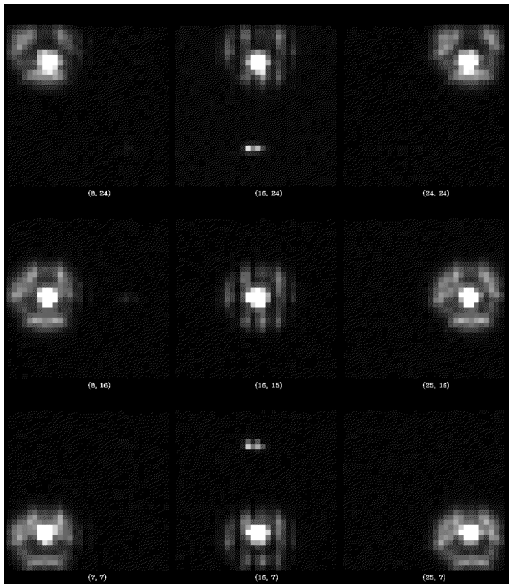

Figure 7: Simulated ghosts images obtained with ASAP when a point source moves over the detector (CVF at 7 μm with PFOV of $6''$) with an artificial gaussian noise. Note the thicker rings of ghosts compared with the observed ones shown in Figure 6 - Koryo Okumura

For the creation of the ghost correction matrix, it is important to consider that the correction may be different for each set of observational data. At the same time, any correction tool has to be made as automatic as possible.

A few cases have already been worked out where it has qualitatively been confirmed that the coherent light simulation does a better job than geometrical optics.

Coherent light simulations create ring-like ghosts for CAM images at 7 and 9 μ and flatter ghosts at 5 μm, which are also observed in real CAM images, although real observations seem to show thinner rings at 7 and 9 μm (see Figures 6 and 7).

Quantitative further refinements of the model are clearly still necessary to assess the accuracy of the possible correction matrix.

BP: Analysis of a possible synchronization problem between ISO pointing files and LWS parallel mode data (July 1999)
Florence Vivares

A shift between the LWS parallel mode data and the pointing files of 0.75 s has been found by Florence Vivares. It has to be noticed here that during operations a similar shift of 0.7 s was also found for the SWS science data and of 0.75 s for the PHT serendipitous mode data. The issue was discussed with Fokker in the past and no complete explanation was found. With the new synchronization problem found by LWS, the issue will be re-opened again.

Glitches:

GL: Advanced modelling of radiation impacts (including production of secondaries) and effect of shielding on the observed glitch rates (august 1999)
Petteri Nieminen

Petteri Nieminen presented at the last WG meeting the results obtained applying the GEANT3.21 Monte-Carlo particle transport simulation code to ISO LWS Ge detectors.

The current work consider the detector shielding structure and physical interactions of the incident protons, including secondary particle production.

The simulation is based on the cosmic ray proton spectrum predicted by CREME96.

Plots of simulated energy deposited (MeV) versus frequency of events and versus integral counts/sec were obtained (see Figures 8 and 9).

The results are consistent with those obtained by S. Eckhard in his thesis work and are very important to simulate radiation effects in other missions (FIRST/PACS).

The main conclusion is that we are still far from understanding what is going on. The discrepancies in LWS glitch statistics with models that were previously reported are confirmed.

We still do not know whether the problem is at the detector level or it is related with the electronics. In both cases it is unlikely that such a strong effects on the glitch rate counting can be produced. One would expect the glitch height distribution histograms to be affected through the conversion factors from glitch height to energy deposited. The largest uncertainty here is the photoconductive gain G. It is interesting to note that already in ground tests the spike height values were smaller than expected from the conversion of particle energy to number of electron-hole pairs. The averaged spike heights measured differed by a factor of four between the two Ge:Ga(u) detectors tested. Different G-values

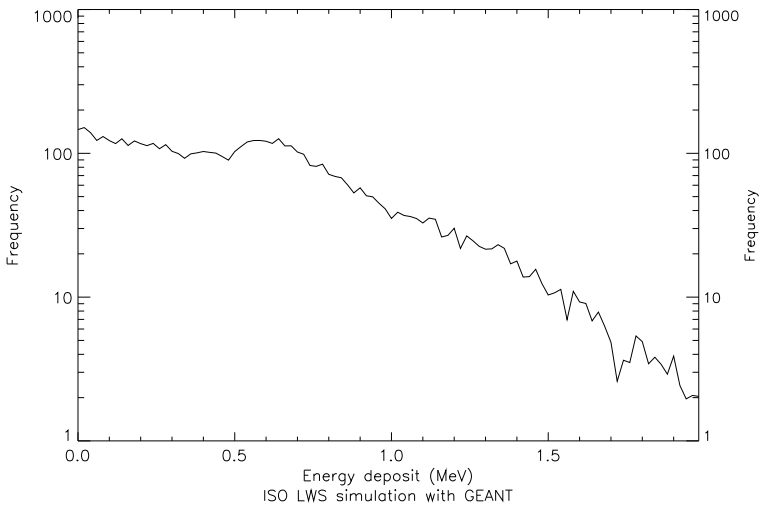

Figure 8: ISO LWS simulation with GEANT: Energy deposited (MeV) versus frequency of events assuming the cosmic ray proton spectrum predicted by CREME96 - Petteri Nieminen

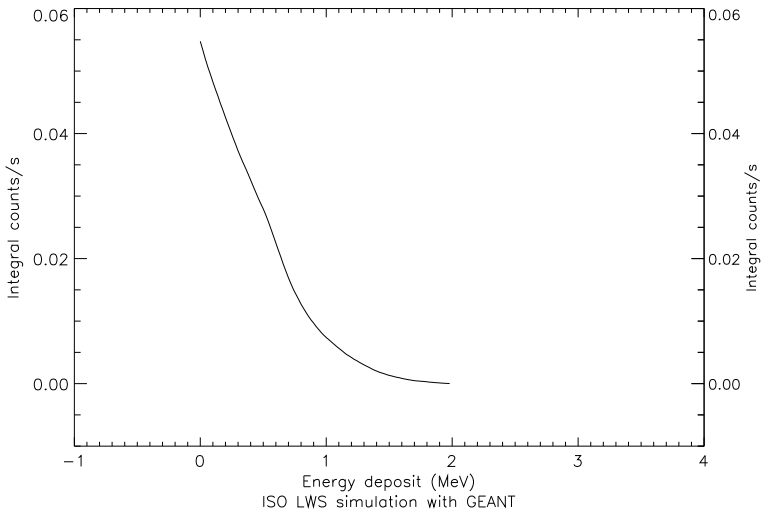

Figure 9: ISO LWS simulation with GEANT: Energy deposited (MeV) versus integral counts/sec - Petteri Nieminen

were assumed to explain these discrepancies (see M. Price's Thesis, sections 5.5.2 and 5.5.4).

Additionally, Martin Burgdorf checked the influence of the dead time after detector resets on glitch rates for LWS. The conclusion is that the dead time is only 55 msec which is equivalent to 11% of a normal ramp length. Hence, all glitch counts should be multiplied by 1.12 (still not enough to explain the discrepancies observed).

GL: Improvements to glitch detection in LWS data (June 1999)

The extension of glitch detection to the *forbidden region* at the beginning of ramps, improving glitch statistics, was implemented in LWS OLPv8.7.

The problem was that glitches affecting the beginning of the ramps were sometimes not considered since these points were discarded as *bad* points before the glitch checking was done. In fact, in some cases large glitches at the beginning of a ramp can produce the detection of an excess of voltage (the glitch tail) for the remainder of the ramp. If these points are discarded then the ramps appears normal and no glitch is detected.

GL: Improvements of glitch detection in SWS data (September 1999) - Helmut Feuchtgruber

Helmut Feuchtgruber presented at the last Glitches WG a list of modules which have been planned to be updated or added to SWS pipeline processing, most likely for OLPv10. Some of them have a direct impact on glitch detection since many of them will lead to a better linearization of the SWS integration ramps. The glitch detection algorithm itself will be tuned by adapting the detector specific calibration files and by fitting a higher order polynome to the data just for glitch detection purposes. A further improvement for glitch detection will be achieved by including the full reset interval for the search for glitches and a cross-talk correction (25% of the glitches in SWS band 4 are due to this effect).

It is obvious that the quality of all these improvements can only be judged at the time they are implemented.

Concerning SWS glitch statistics, Ana Heras made an analysis of the possible influence of saturating glitches, which are discarded in the pipeline, on SWS glitch statistics. The main result found is that they play a minor role. Only 3% in the Si:Ga bands and 9% in the Ge:Be bands are saturating glitches not included in glitch counts.

The full report can be found at:

`ftp://astro.estec.esa.nl/pub/aheras/iso_gwg/glitches_satur.ps`

GL: PACS radiation effects simulations - Helmut Feuchtgruber

Helmut Feuchtgruber reports that no further experiments/simulations with PACS detectors have been performed since the previous meeting. As soon as realistic detector data is available, specially information on glitch tails, work can continue.

GL: Monte-Carlo simulations of radiation effects on ISOCAM
(September 1999)
Arnaud Claret + Herv\'e Dzitko

The results of Monte-Carlo simulation of radiation effects on ISOCAM were presented by Arnaud Claret at the last WG Meeting. The simulation takes into account a galactic proton spectrum, the ISOCAM geometry and particle interactions to derive the glitch characteristics.

Using a simple model of the ISOCAM geometry, synthetic glitches were produced using GEANT code for different conditions (see Figure 10).

The glitch size, glitch rate and energy properties can be predicted this way and compared with in-flight data.

A mean number of 8.48500 $\pm$ 0.459757 pixels/glitch and a glitch rate of 0.831274 $\pm$ 0.124441 glitches/sec are derived.

Experimentally, $\sim$1 glitch/sec is detected, close to the mean value (if we consider the errors) of $\sim$0.83 glitches/sec derived.

The contribution of secondary particles to the total number of events observed in LW detectors was also analysed by Hervé Dzitko. With the assumed simple geometrical model we can consider a shielding which represents a total absorber thickness roughly equivalent to 25 mm of Al. Under these conditions only particles with larger than 6,75 g/cm^2 can reach the detector. 80 Mev protons can traverse this shielding as well as 80 Mev/nucleon Alphas.

Using data provided by KET on board Ulysses a number of 0.36 tracks per second due to galactic cosmic ray protons and alphas are expected to pass through 8 pixels of the detector on the average.

Counting rates induced by secondary nuclear interaction particles can be estimated through an analytical approach, assuming the geometrical interaction cross section and the average multiplicity of the interaction, and considering also the secondary particles emitted by the shield near the detector.

Taking into account the Galactic cosmic ray composition, primary particles should produce a 20% of additional counts due to nuclear reactions in the shielding and a 25% of additional counts would be the contribution of the body of the satellite. In addition, δ-rays provide an additional counting of 32%.

Therefore, primary particles should produce about 75% of additional events either by nuclear reactions or *delta*-ray emission.

In addition, the thorium radiactive lens (not considered) may affect the statistics and account for $\sim$16 glitches/sec. This is an anti-reflecting coating of

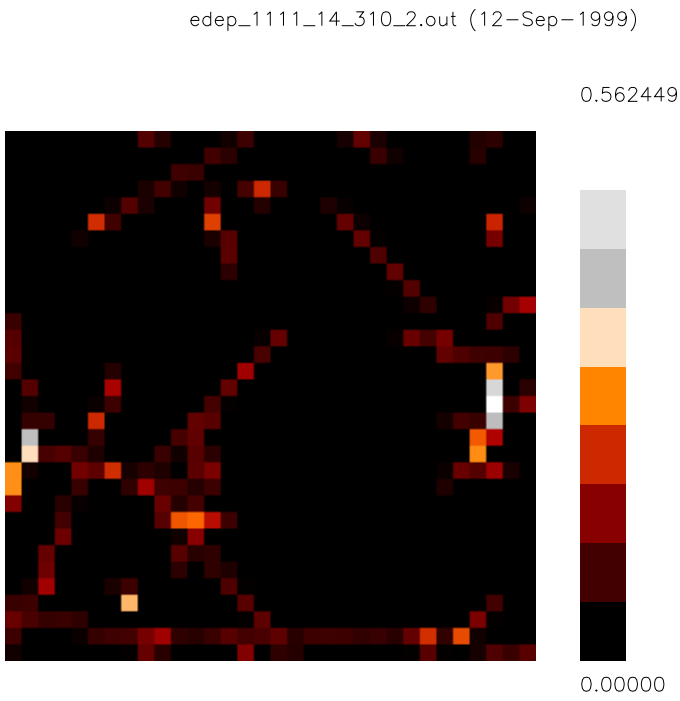

Figure 10: Example of synthetic glitches produced using the GEANT code applied to CAM data - Arnaud Claret

the 6″/pixel lens. Glitches produced by this radiactive lens would be point-like (i.e. 1 or 2 pixels/glitch instead of 8 pixels/glitch for those induced by isotropic protons).

In summary:
- Primary particles contribute with 0.36 counts/sec
- Secondary particles contribute with 0.27 counts/sec
- Th radiactivity contributes with 0.16 counts/sec

which gives a total number of 0.79 counts/sec.

GL: Investigation on new de-glitching methods for ISOCAM data (September 1999)

Stephan Ott

Several new de-glitching methods were presented by Stephan Ott at the last WG Meeting for application to ISOCAM data.

The following de-glitching methods were described:
1. MMMS (Multi-Method, Multi-Step)
2. Sky-cube de-glitching
3. BISC (Best Iterative Sigma-Clipping)
4. NOSC (Normalised Sigma Clipping)
5. Clipper

The idea is to take advantage of valuable information about ISOCAM's current configuration, glitch distribution, flux level and redundancy in the raster or beam-swith observation, ignored by currently existing standard de-glitching techniques (multi-resolution, sigma clipping,...). This leads to badly chosen thresholds, which result in too high noise level due to un-suppressed glitches, masked out sources or gradients and no deglitching for observations with few read-outs.

Example of results obtained with each method were shown (see Figure 11) and a list of application fields and caveats to take into account. All of them give very satisfactory results. In view of this, the Glitches WG strongly recommends to investigate the possibility of inclusion of one or more of these algorithms in the CAM pipeline, although it requires a detailed and careful study of the problem, since it would require the application of *blind* corrections to the data.

GL: Implementation of a new de-glitching method in PHT pipeline (February 2000)

Concerning PHT, and as already reported in the previous Status Report, the implementation of the new, more sophisticated, de-glitching method which works at ERD level in the pipeline was postponed to OLP version 10.0 since it requires a quite different approach to the problem (the correction is applied at read-out level and not at ramp level).

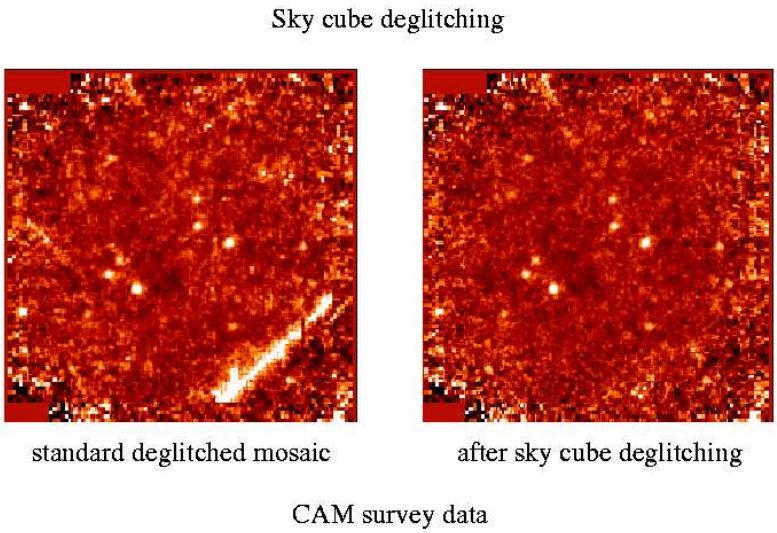

Figure 11: Example of results obtained after application of the Sky-cube deglitching method to ISOCAM data - Leo Metcalfe

Line profiles:

```
LP: Determination of the SWS spectral resolution and instrumental
     line profile as measured by the full resolution modes  SWS02
     and SWS06. Final results (September 1999)
        Dieter Lutz
```

The last version of the document *ISO-SWS grating resolution and instrumental line profile as measured by the full resolution modes SWS02 and SWS06* by D. Lutz, H. Feuchtgruber and J. Morffin will soon be posted in the external ISO web.

The document has been significantly updated although some of the values presented should be considered subject to further modifications. It includes a description of the database used and existing models for the SWS spectral resolution. In addition, an analysis of the effect of rebinning and extension of the source observed on the spectral resolution is presented. The reproducibility, observed trends with time and the possible dependence of resolution on detector, line flux or continuum flux are also investigated.

For most practical purposes, it is completely adequate to assume that an SWS instrumental profile is intrinsically a gaussian. The document gives a formula to estimate the expected line width as a function of source extent.

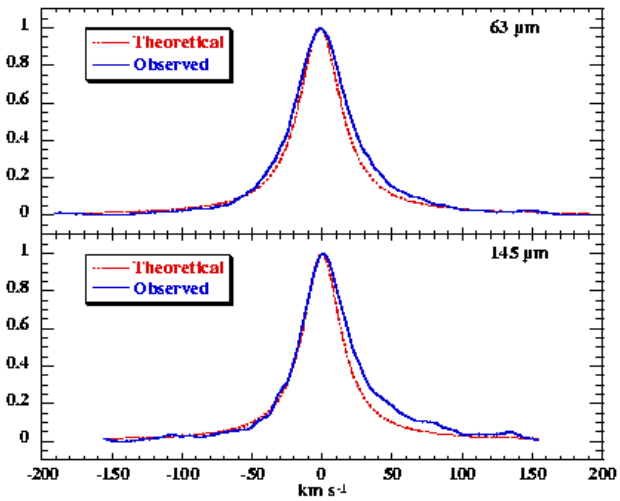

Figure 12: Theoretical and observed Fabry-Pérot line profiles at 63 and 145 μm. Note the asymmetries probably due to memory effects. - Emmanuel Caux

Other effects like mispointing, ghosts and transients are also discussed in the document.

Future plans include the extension of the analysis to other sources increasing the database and the implementation of a cross-talk correction which might explain the broad wings observed at a few per thousands level.

`LP: Progress on analysis of LWS line profiles (September 1999)`

The study of the LWS grating profile has been completed for point sources and short wavelength detectors by Rosario Lorente. The result is a single profile valid for all SW detectors. Unlike SWS, LWS line profiles deviate slightly (∼4%) from a gaussian shape. The error made on the flux determination by using a gaussian fit is of the order of 2%.

The asymmetry found in the 57 μm line in the SW2 detector is still being studied in relation to the presence of an unidentified line (or feature) in the Fabry-Pérot spectra.

The line profile analysis has now been extended to the long wavelength (LW) detectors and again the preliminary results indicate slight deviations from gaussian shape (∼5%).

In the near future, the line profile analysis will also be applied to extended sources.

The ultimate plan is to produce mean profiles and specify their domain of validity. The grating profiles will be compared with gaussian profiles and

recommendations will be given to users on how to analyse LWS grating lines.

The LWS grating profiles have also been compared to pre-launch ray-tracing results at 45 μm by Anna di Giorgio. The agreement found is very good at the top of the line although the base of the line is wider than predicted.

Concerning the LWS Fabry-Pérot profiles, they have been derived by Emmanuel Caux for several lines (52 μm, 57 μm, 63 μm, 88 μm, 122 μm, 145 μm and 158 μm) on three objects (G0.6−0.6, NGC 7023 and NGC 7027), observed with the standard AOT LWS04. They compare very well with the theoretical profiles apart from an asymmetrical widening probably due to memory effects, although a misalignment (if the tilt has been changing during the scan) could also produce a similar effect (see Figure 12). The origin of this asymmetry is currently being studied by Anna di Giorgio using COIF observations performed with both forward and backward scans which will be compared the with standard LWS04 observations (for which only one scan direction was used) of the same object.

It is foreseen that a tool will be provided in LIA to fit the FP spectra with the derived profiles.

Photometric calibration:

General:

The old *Calibration Liaison* web pages, used during the mission for posting (cross-)calibration information originally intended for internal use only by the ISO Calibration team have now been updated by Pedro García-Lario. The intention is to make the information there contained available to the ISO users community as part of the ISO Data Archive.

For the time being these new *ISO Calibration* web pages (see Figure 13) are still only accesible through the internal Web server (pending a few proprietary issues) but soon they will be posted in the external ISO web.

They will contain detailed information on the calibration standards on which the absolute flux calibration of ISO is based. This includes a description of the ISO Ground Based Preparatory Programme (GBPP) and the Cohen, Walker, Witteborn et al. (CWW) absolute calibration programme, as well as information on the asteroids and planets that were used for the calibration at longer wavelengths. Photometric and spectral data are provided together with model spectra of the different ISO calibrators and the definition of the system zero-points.

These pages will regularly be updated with additional information and improved data when it becomes available.

ISO Calibration

The calibration of ISO data

Definition of ISO calibration standards

Stars

The absolute flux calibration of three of the four ISO instruments (CAM, PHT and SWS) is based primarily on results obtained on stars selected from the ISO Ground-Based Preparatory Programme (GBPP) and from the Cohen, Walker, Witeborn et al. (CWW) absolute calibration programme. The confidence in the absolute flux level of the calibration stars is about 3% in the 2.5 to 35 microns wavelength range and better than 10% at longer wavelengths up to 300 microns.

Asteroids

Asteroids are used to cover the 35 to 200 microns wavelength range in ISO calibration since stars are usually too faint to be used in this wavelength range. An extensive ground and airborne based calibration programme was carried out to quantify the fluxes and to monitor the light curves of the prime asteroids 1 Ceres, 2 Pallas, 4 Vesta, and 10 Hygiea, and other asteroids that have been observed with ISO. For the current calibration the absolute fluxes of the asteroids were derived using a thermophysical model (Mueller and Lagerros 1998). The accuracy of the predicted asteroid fluxes is in general 10% in the wavelength range from 24 to 500 microns.

Planets

The outer planets Neptune and Uranus were used for calibration at the longer wavelengths in the high flux density range up to 1000 Jy. The model SED's for a given time in the mission were provided by M. Abbas. Currently, the absolute flux calibration of LWS is based on Uranus as primary source. Comparison with independent model predictions for Uranus showed a consistency of better than 20% in the wavelength range between 30 and 240 m. At shorter wavelengths the models become less certain.

Photometric and spectral data

Results from the ISO Ground-Based Preparatory Programme (GBPP). They consist of near and mid-IR photometry of a wide sample of stars observed from La Palma (P. Hammersley) and ESO-La Silla (N. van der Bliek, J. Manfroid and P. Bouchet) observatories.

Results from M. Cohen et al., including calibrated spectra and extrapolations to 300 microns for a few stars.

Models

Models of Uranus and Neptune

Model spectra of stars in the Ground Based Preparatory Program. The visible magnitudes and near-infrared photometry observed in the GBPP have been fitted with a Kurucz model to provide the flux densities at longer wavelengths. The overall spectral energy distribution is believed to be correct within 5% .

Model spectra assembled from ground-based and KAO observations from M Cohen et al.

Definition of the system zero-points

The model spectra of Vega (1-300 microns, R = 4000 throughout, 400 kB) provides the definition of the system zero points (by adoption of the ideal [i.e. model] Vega as zero magnitude in every passband) so that long wave measurements can be quoted in magnitudes or at least with reference to a common context as measurements at other shorter wavelengths. See also explanatory note for details.

The model spectral energy distribution of Sirius (1-300 mic, R = 4000 up to 35 microns) is also available. This star was also considered a primary reference star for calibration purposes.

Other documents

Cross-calibration

- ISO Post-Operations Cross-Calibration Status Report, SAI/1999-060/Rp, (07-Jun-1999)
- ISO Cross Calibration Plan (June 1999)
- "Reference wavelengths for ISO CAM and PHOT filters" by A. Moneti, L. Metcalfe and B. Schulz, SAI/97-002/Dc (15-Sep-1997)

Please send corrections, comments and suggestions to Pedro Garcia-Lario
(Last update: 23-08-1999)

Figure 13: The introductory new ISO Calibration web page

Concerning photometric calibration of extended emission versus point sources, Alberto Salama reported at the last Photometry WG meeting that beam profiles are now available for all instruments allowing extended emission flux calibration. This is expected to have a significant impact and represents an important improvement in the photometric analysis of extended sources. Comparisons between different instruments, however, can still be very difficult when the extended emission is structured as with the aperture measurements it is only possible to derive an integrated value over the beam profile (with the exception of CAM, where spatial information on the source can be obtained).

The improved pointing correction implemented in OLPv8.6 (see *Beam Profile/Pointing WG* subsection) will also lead to a significant improvement in absolute flux calibration. Correction tools and/or new calibration files which consider the combination of the pointing information with the beam profile, are being produced by the different instrument teams which will improve significantly the absolute photometry.

The effect is expected to be specially important for SWS and PHT data. For SWS, new Cal-G files have already been produced by Rosario Lorente which correct for this effect and they will be implemented in the next version of SWS IA. The application of this correction to SWS data is expected to elliminate the mismatches sometimes observed between different bands for bad-pointed observations and minimize the jumps between bands in SWS observations of extended sources.

In the case of PHT, the correction tool has recently been implemented in PIAv8.1. Tests are still on-going, but the application of this correction should lead to significant changes, both in intensity and spectral shape for bad-pointed observations and/or extended sources.

The latest progress reports on absolute flux calibration of individual instruments were also presented at the last meeting of the Photometric Calibration WG.

- **PHT:**

  The correction for the non-linear behaviour of the PHT detectors is one of the major upgrades successfully implemented in the new version 8.4 of the pipeline (released in August 1999).

  The impact of such non-linearity on the flux calibration and the method used to correct for this effect are discussed in the document *Linearization of ISOPHOT-P and C detector signals in OLP8* by Bernhard Schulz which can be found at:

  `http://www.iso.vilspa.esa.es/users/expl_lib/PHT/r_nonlin.ps.gz`

The response of the PHT detectors is found to be dependent on inband power. A remarkable (and not understood) aspect is that this behaviour is also filter dependent, showing even opposite trends for the response versus inband power. The adopted correction is used for all AOTs except for PHT40 (PHT-S spectra).

Another important change in OLPv8.4 of the PHT pipeline is the new signal derivation and calibration of chopped measurements. An updated Spectral Response Function (SRF) is available for PHT-S chopped measurements, which contains a correction term dependent on the signal difference, which allows to correct for signal transients typical for this flux step.

The FCS calibration files were derived once more for OLPv8, now based on the final complete data set of calibration measurements acquired during the mission, with the calibration curves now including the flux dependent signal linearization. Consequently, revised limits of validity resulted.

In addition, new effective solid angles for PHT-S, including the extension of the beam beyond the physical PHT-S aperture size (axis radius = 12") are available. With these new solid angles, PHT-S measurements of diffuse Galactic light were compared to IRTS/MIRS spectra showing a good agreement on the absolute flux level, although a deviation exists around 10 μm.

New determinations of the PSF fraction on the arrays (C100 and C200) are now used (see *Beam Profiles/Pointing WG* subsection). Examples of photometric measurements on alpha Bootis and Arp 220 gave clear improvements when compared to the models.

Additional information on the impact of each of these upgrades in the calibration accuracy of PHT is given in Section 4 of this document.

- **SWS:**

  An overview of on-going calibration work for SWS was given by Russ Shipman at the last WG meeting. An important piece of work at this moment is the correction for memory effects (transients). This is at the moment becoming available for band 2 (see next *Transients WG* subsection). Work started for band 4, but the behaviour there is very different and the question remains whether a good model can be found for it.

  Russ Shipman is also investigating a new approach to determine the gains of the detectors to reduce the noise in a different way. Instead of determining the gain for each individual detector, the whole array is used. Work is on-going on this subject.

- **CAM:**

  Although the flux calibration of CAM is based on the observations of standard stars, a recent work done by Francois Boulanger shows that there is good agreement between the CAM filter measurements on the zodiacal

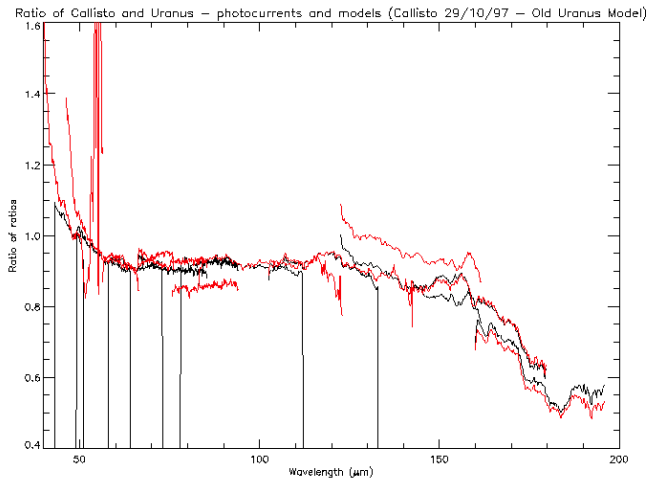

Figure 14: Ratio of ratios Uranus/Callisto observations versus Uranus/Callisto model (red line for Uranus new model and black line for the old Uranus model). Note the strong discrepancy below 50 μm and beyond 100μm and the good agreement between 50 and 100 μm - Bruce Swinyard

background and the predictions by the ZODI model which is based on DIRBE observations. This indicates that the calibration of point and extended sources agree. However, strong deviations are found when comparing the CVF measurement with the ZODI model. There is a minimal offset of 10% but it can be 30% around 10 μm. The difference is explained by a contribution of reflected light (the so-called *ghosts*) which is wavelength dependent.

- **LWS:**

  The flux-calibration of LWS is hampered by the uncertainties in the models of planets. At present the absolute flux-calibration is only based on Uranus. Martin Burgdorf presented at the last WG meeting comparisons of observations of other solar system objects with the available models.

  The comparison with Mars showed discrepancies up to 10-15 wavelengths. Mars, however, is much brighter than Uranus and had to be observed in a non-standard way (low bias) which may cause the observed differences.

  For that reason a comparison with Callisto was made (see Figure 14), since Callisto is of a more comparable flux density to Uranus. The agreement between 50 and 100 μm is quite good (less than 10% deviations), but there is still a discrepancy below 50 μm (see discussion on this later under the *Spectral Matching WG* subsection) and at longer wavelengths than 100 μm, where straylight caused by Jupiter in the Callisto spectrum is

expected. A correction for this straylight effect will be applied soon.

Another comparison with Neptune gave good agreement. Further study of the Neptune model by comparing with groundbased, PHT-S and CAM-CVF measurements is on-going.

Cross-Calibration:

```
PH: Definition of selected sample of targets (stars, clouds,
    galaxies, ...)  on  the  basis of  specific calibration
    problems under  analysis for cross-calibration purposes
    (September 1999).
       Pedro Garcia-Lario
```

The new *statistical* Cross-calibration strategy described in the previous Status Report has been activated. The first step has been the selection of a sample of a few hundred sources observed in at least two of the following AOTs: SWS01 (low resolution spectroscopy), PHT40 (PHT-S staring or chopped measurements), or CAM04 (CAM-CVF spectrophotometry). The goal is to evaluate the internal consistency of ISO calibration for sources observed with these three instruments in the overlapping region from 2 to 15 μm. The sample includes a variety of blue and red objects, faint and bright, and of course point-like and extended sources, which makes it ideal for studying the various calibration problems affecting each type of object observed with ISO.

The preliminary results obtained so far are presented and discussed in Section 3.

The future plans include the extension of the same kind of analysis to longer wavelengths. In this sense, a second sample of objects observed with both PHT-C filters (photometry beyond 60 μm) and LWS01 containing a few hundred different pointings has already been selected from the ISO Data Archive. The main problem is, in this case, that cross-calibration comparisons are difficult in many cases because the dynamic range of PHT and LWS is very different. Thus, there is a minimum overlapping region in flux level at which both PHT and LWS are of enough quality to derive reliable cross-calibration comparisons. In spite of this, we estimate that a minimum number of 50 cases will probably remain as useful.

In addition, the ISO calibrated data will also be compared with non-ISO data (IRAS, KAO, COBE,...) at a later stage. There are plans to at least combine colour-corrected IRAS fluxes with spectroscopic data obtained with ISO (SWS+LWS) in the near future. The results from these cross-calibration comparisons will be presented in the next version of this Status Report.

PH: Evaluation of calibration improvements recently achieved and investigation on cross-calibration problems reported in the last Status Report affecting OLP and/or IA data with special emphasis on OLPv8 data products (November 1998)

See Sections 3 and 4 of this document for a detailed report on the evaluation performed and results obtained.

Polarisation:

PO: Workshop on "ISO Polarisation Observations" held at VILSPA (May 1999)

The aim of the meeting was to support the finalization of data reduction and analysis of observing programmes based on polarisation measurements carried out with ISO.

The analysis of polarisation measurements requires expertise in advanced data reduction techniques and a deep instrument knowledge.

The workshop was an excelent opportunity for astronomers working on this particular field to access the latest calibration updates with the support of the IDC staff during *hands-on* sessions and at the same time exchange scientific results with other colleagues.

15 astronomers attended the Workshop held at VILSPA from May 25 to 28, 1999. The final programme can be found at:

http://www.iso.vilspa.esa.es/meetings/polarisation/final_announcement.txt

The proceedings of this Workshop are available at:

http://www.iso.vilspa.esa.es/meetings/polarisation/paper/web/

As an outcome of the ample discussions held during the Workshop conclusions were reached on the orientation of the CAM polariser which, as it is now defined, looks convincing and provides consistent results on polarisation angles. However, the general feeling was that still a better de-glitching strategy is needed to improve the results obtained and that downward transients are insufficiently corrected in the data with the available detector models.

Concerning PHT, for extended sources the C200 2x2 raster polarisation maps give still inconsistent polarisation angles for the central pixel of the resulting

3x3 pixel map, which is covered by all 4 pixels. René Laureijs and Ulrich Klaas are searching for a solution.

Following the meeting, a new de-glitching strategy on CAM05 data has been tested by Ralf Siebenmorgen which looks very promising. Further testing is on-going, using fine-tuned polarisation flat-fields and new polarisation weight factors with the help of this new de-glitcher.

```
PO: Analysis of the PHT polarisation inconsistencies among the
     C200 pixels (September 1999)
        Rene Laureijs
```

Re-calibration of PHT instrumental polarisation by including the new linearity correction seems to give better results for discrepant pixels. However, additional investigation is still needed.

Spectral Matching and RSRF:

```
SM: Comparative study of cross-calibration tools: Atlas/IDA/UDF/PIA/ISAP
     (July 1999)
        Alberto Salama/Pedro Garc\'\i a-Lario
```

In the previous Status Report the problem of selecting an adequate tool to be used for cross-calibration purposes during post-operations was addressed. The situation has not changed too much since then. In summary, the ideal cross-calibration tool should:

- be able to cope with a large number of data sets both of OLP and IA data products indistinctly in a fast and simple way.
- allow some basic manipulation (change of units, scaling, basic statistical analysis) of the data.
- provide the user with powerful (over-)plotting capabilities.

Several possibilities have been investigated:

- **SPDT:** Unfortunately, the ISO Survey Products Display Tool (SPDT) recently released as part of the ISO Data Archive v3.0 do not allow the possibility of overplotting data corresponding to more than one observation, nor to carry out synthetic photometry on survey data products or other similar functionalities. However, it is very useful for a quick first look at the data.

For single wavelength CAM images it is possible to:

- manipulate the colour table in single wavelength CAM images
- identify J2000 sky coordinates
- zoom in and out

For LWS, SWS and PHT-S spectra it is possible to:

- select different detectors individually
- manipulate x-axis and y-axis scaling input fields
- manipulate x-axis and y-axis selecting a region using the mouse

- **ATLAS:** This is an IDL-based tool developed by Ekkehard Wieprecht and Alberto Salama which allows direct comparison of SWS and LWS ISO survey products. From an input list of TDT numbers created with an SQL query to the ISO Data Archive, it provides $m \times n$ plots on single pages for easy comparisons of a number of targets. Some IDL post-processing is also carried out by the Atlas tool like flux units conversion and automatic scaling for pairs of SWS-LWS spectra on the same target. Although it could be extended to PHT and CAM data with some additional manpower in its present form it is only useful for the investigation of SWS/LWS cross-calibration aspects.

- **PIA:** Display tools currently exist under PIA that can easily be adapted to ingest and allow the overlapping of data corresponding to other instruments. This can be implemented with a small manpower effort. It would be desirable to have ready this possibility soon to deal with PHT, CAM and SWS cross-calibration comparisons. Our recommendation is to encourage the implementation of these small changes in PIA.

- **UDF:** Under development by E. Wieprecht and E. Wiezorrek, the User Defined Function (UDF) will soon be installed within the ISO Data Archive. This facility allows to query meta-information contained in a given observation. With a series of User Defined Functions it will be possible to extract virtual attributes from files external to the database engine. These virtual attributes can then further be used in queries inside the database engine. Eventually, when the necessary changes will be incorporated into the S/W, it will be possible to properly handle not only OLP data, but also data processed with any of the four instrument IAs. Thus, our final recommendation is, on a longer time scale, to encourage the use the UDF facility as the main tool for future cross-calibration comparisons.

- **ISAP:** The photometry option of ISAP is currently able to read in not only SWS and LWS data but also CAM-CVF, PHT-S spectra, IRAS data and soon SIRTF data, and thus can also be used for cross-calibration purposes.

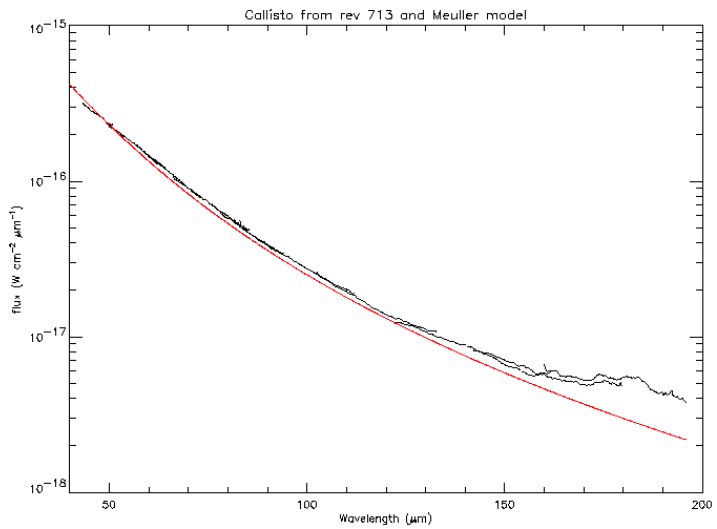

Figure 15: New thermophysical model of Callisto (in red) compared with LWS observations of Callisto made in revolution 713. The agreement is always within the 15% level except beyond 150 μm due to straylight from Jupiter - Thomas Müller

```
SM: Investigation on  SWS/LWS mismatches.  Identify possible role of
     extended and variable emission to explain the discrepant values
     found (July 1999)
        Pedro Garcia-Lario
```

In the previous Status Report we presented the preliminary results of a cross-calibration analysis of bright sources observed both with SWS and LWS at 44 μm. The sample was selected from the ISO Data Archive by Alberto Salama and the discrepancies found have been further investigated by Pedro García-Lario.

The main conclusion is that they can always be attributed to either the variable nature of the sources or due to the their extended nature, which leads to different fluxes as the apertures of LWS and SWS are different. A more detailed description of the analysis carried out and results obtained is presented in Section 3 of this document.

```
SM: Definition of a thermophysical model for Callisto (July 1999)
        Thomas Mueller
```

A new thermophysical model of Callisto has been produced by Thomas Müller. Callisto was selected as an independent calibration source for LWS

to be compared for sanity check with Uranus as an alternative to Mars because it shows a more comparable flux density.

The thermophysical model of Callisto shows a reasonable agreement with SWS/LWS data (see Figure 15) at most wavelengths.

The discrepancy observed beyond 150 μm is interpreted as due to contribution from straylight from Jupiter.

A smaller discrepancy is also observed at the short wavelength end of LWS (SW1 detector) which is still being investigated. A possibility could be that a real feature exists at this wavelength in the spectrum of Callisto. However, again a similar effect was previously observed in Neptune and other solar system objects, which makes this possibility unlikely. Moreover, the effect is not observed at all in band 4 of SWS, where there is a perfect match with the model.

In general the conclusion is that Callisto's spectrum is well suited for checking the flux calibration of LWS at least in the spectral range shortward of 100 μm (before a satisfactory correction for the straylight effect from Jupiter is applied).

```
SM: Definition of the RSRF for SWS; determination of the level
     of accuracy (September 1999).
        Bart Vandenbussche
```

The full report can be found in *The ISO-SWS Relative Spectral Response Calibration* by Bart Vandenbussche at:

```
http://www.iso.vilspa.esa.es/users/expl_lib/SWS/rsrf_v1.1.ps.gz
```

This document describes the different corrections that were applied in different versions of the pipeline to the SWS RSRF and indicates where further improvements can be expected.

Before launch, the SWS RSRF was derived from black-body scans during ILT tests. Uncertainties in black-body temperatures, diffraction losses and leaks in test set-up filters made a correction in the RSRF necessary, based on what it was observed in-orbit on external calibrators.

The impact of incorrect RSRFs on the final spectrum after a slightly wrong dark current subtraction is discussed and methods to recognize and cure the problem are provided.

As an example, a sudden fall-off at the blue edge of bands 1a and 2a systematically observed in all observations was identified as produced by a leak in ILT set-up filters. The effect was corrected in May 1996 in the corresponding RSRFs by comparing the spectrum of Alpha Lyrae (a representative case) with a model spectrum provided by Martin Cohen (see Figure 16).

Additional corrections were needed to correct for diffraction losses effects derived from the fact that the black-body sources observed in the ground were extended with respect to the SWS slit and not point sources.

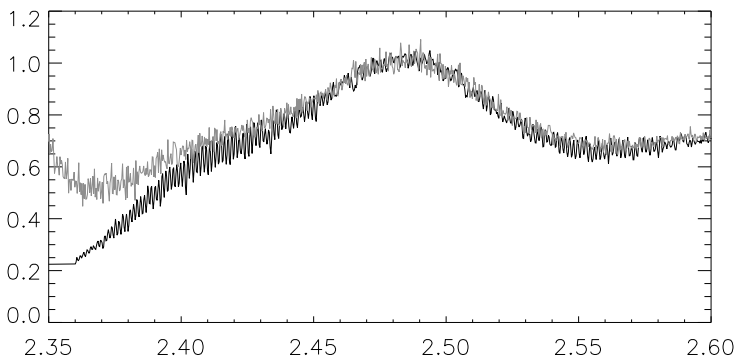

Figure 16: The difference between the RSRF before (black) and after (grey) the first in-orbit correction for SWS band 1 - Bart Vandenbussche

In March 1997 new Cal-G files were obtained by applying polynomial corrections to the existing files, based on the differences between SWS spectra of standard stars and reference spectral energy distributions, mostly synthetic spectra and composites (i.e. pieces of synthetic spectra and real data spliced to accurate photometry available).

In the fall of 1997 a new set of RSRF calibration files were derived using more data of known calibration stars with a better sampling of different spectral types. Cross-talk correction was this time considered, as well as a better wavelength calibration and dark current subtraction. Unfortunately, a lack of calibration targets with a well known energy distribution in the region 30–45 μm, no correction was applied on the RSRF for band 4.

Several features are identified in the document provided by Bart Vandenbussche which might be instrumental effects produced by residuals in the RSRF. The most important problems in the RSRF can be summarized as follows:

- Band 2C: 9-9.3 μm : possible residue of the correction for the instrumental absorption feature.
- Band 2C: 10.1 μm : possible residue of the correction for the instrumental emission feature.
- Band 2C: 11.0 μm : possible residue of the correction for the instrumental emission feature.

- Band 3A: 12.3 μm : possible residue of the correction for the instrumental emission feature.
- Band 3A, 3C, 3D, 3E : the fringes in bands 3 were also observed during the instrument level tests, so they are also present in the RSRF and will be divided out. However, the fringes in the RSRF are less resolved than in high resolution observations on point sources since the blackbody in the lab was extended to the SWS slit. Slight pointing errors will also result in a wavelength shift of the spectrum observed, so that the fringes can be slightly shifted with respect to to the fringes in the RSRF, and this will result in fringe residues in the spectra.
- Band 3D: the red side of band 3D shows leakage from the wavelength region around 14 μm. Since the RSRF was corrected based on observations of stars that have a relatively high flux at 14 um, no proper correction of the RSRF in the leakage region was applied. In spectra of cold sources a false drop at the end of band 3D can be seen.
- Band 4 : no in-orbit correction has been applied due to lack of suitable observations/sources. It is now known that the lab measurements show a strong de-biasing effect, and it can thus be expected that the shape of the current band 4 RSRF has a global inaccuracy of about 10%.

The steep slopes shown by the SWS RSRFs in some spectral regions can induce false shapes in the calibrated spectra. Poor matches between different AOT bands can often be understood (and corrected for) from a combination of a wrong dark current subtraction and a steep slope in the RSRF at a given wavelength. Note that 10% is typically the difference between two dark current mesurements in an observation. Thus, it is reasonable to expect mismatching problems of this order specially where the signal level of a scan is of similar strength than the dark currents for that band.

Improvements in the RSRF calibration of SWS are expected in the following areas:

- Use of new and improved synthetic spectra.
- Extrapolation of the correction in the leakage region at the red side of band 3D, since verification on cold sources has shown that an extrapolation of the correction factors is better than no correction.
- Re-derivation of the RSRF for band 4 with proper de-biasing correction of the ILT data. De-biasing has shown to be important at the signal levels of these data.
- Re-derivation of the RSRF band 2 with proper memory effects correction of the ILT data.
- Re-derivation of the RSRF for all bands with improvements in the calibration at the slope level.

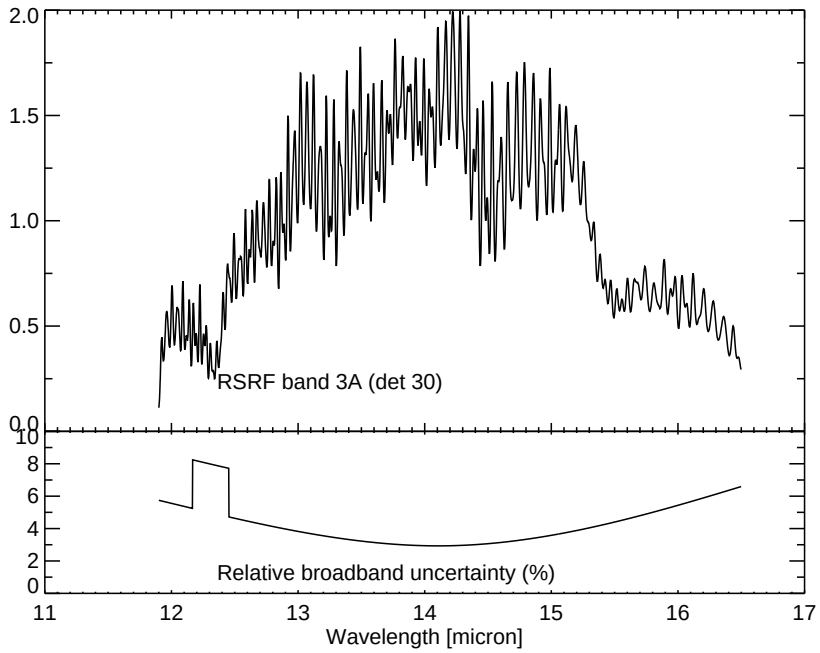

Figure 17: The RSRF for SWS band 3A (top) and relative broad band uncertainty (bottom) - Bart Vandenbussche

SM: Progress on the definition of a new RSRF for LWS based on Uranus observations (November 1999)
Martin Burgdorf

Helmut Feuchtgruber presented at the last Spectral Matching WG Meeting an SWS spectrum of Mars after correction for de-biasing. The continuum has changed with this procedure by 15–20%. The de-biasing constant is found to be 3.5; this value was derived from the deviations from linear ramp shapes. As the conditions for SW1 in the LWS are similar, the same effect would be expected there but this is not seen.

A comparison between Uranus and Mars spectra observed at nominal bias was carried out by Bruce Swinyard using both the old (March 1996) and the new (October 1996) Uranus models.

The continuum flux from the low bias observation of Mars corresponds to an emissivity of 0.79 whereas the observation at nominal bias suggests a value close to 1 (see Figure 18).

There are two possible explanations for this discrepancy: The responsivity is different for different flux levels, therefore the absolute flux calibration is not valid anymore for an object as strong as Mars, or the debiasing effects are stronger at reduced than at nominal bias, which can be discarded. It is also

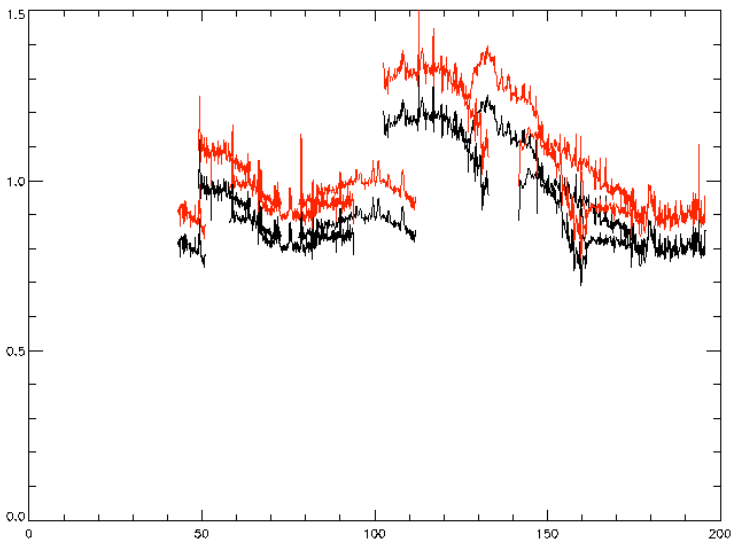

Figure 18: Comparison between Uranus and Mars spectra at nominal bias. (red: Mars emissivity = 0.98; black: Mars emissivity = 0.79) - Bruce Swinyard

possible that the new Uranus model is incorrect at the short wavelength end, but more work will be required to sort this issue out.

Finally, the observed spectrum of Neptune has been compared with a model by G. Orton with a brightness temperature a few degrees higher than what it was assumed before.

Figure 19 shows that the new model agrees well with the LWS data in photometric mode and with the SWS data from band 4 when an offset of 20 Jy is added (see Figure 19). This offset is needed to bring the SWS spectrum in agreement with LWS in the overlapping region. Note that the size of this correction is smaller than the uncertainty of the dark current. Actually, the raw data should have been re-run through the pipeline with a lower dark current, since a simple shift assumes a constant relative spectral response function, but the error caused by shifting only is expected to be negligible.

Transients:

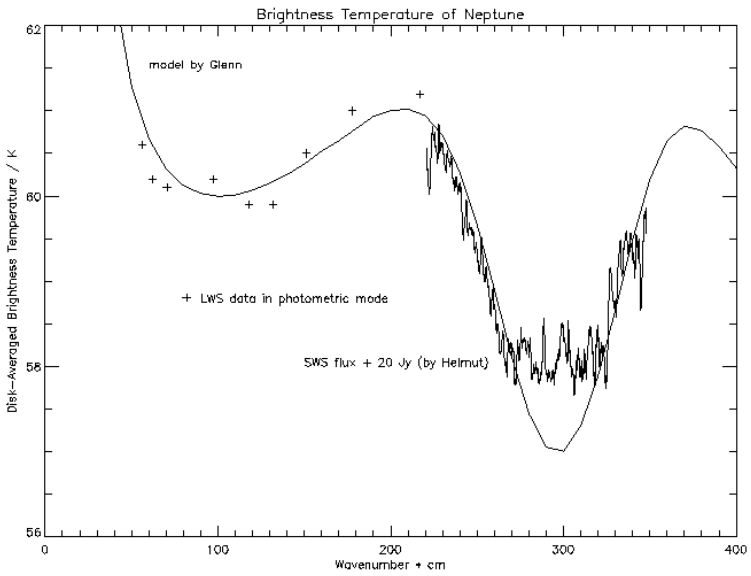

Figure 19: Comparison of the Neptune spectrum with a model by G. Orton. Note the nice agreement when an offset of 20 Jy is added - Martin Burgdorf

`TR: Transients correction tool based on the Fouks-Schubert method for SWS data available under OSIA (September 1999)`
`Fred Lahuis + Do Kester`

Fred Lahuis presented the latest news concerning the implementation plans of transient corrections into SWS IA, OSIA and SWS pipeline.

The adapted Fouks-Schubert method applied to band 2 (Si:Ga) SWS data developed by Do Kester is working very well. It will be implemented in the next SWS IA version. Later it will be incorporated into OLPv9.5 (release expected September 2000) and into OSIA.

For SWS band 4 (Ge:Be), however, the Fouks-Schubert method does not work and there is no alternative working model yet. Efforts are on-going to find an alternative method.

`TR: Applicability of Fouks-Schubert transient correction to the various types of detectors on-board ISO (October 1999)`
`Alain Coulais`

The applicability of the Fouks-Schubert method to the various types of detectors on-board ISO can be discussed in terms of the E_j parameter which basically depends on the quality of the contacts in the detectors under study.

Fouks-Schubert model can be used when $E_0/E_j >> 1$.

It is found that for the Si:Ga ($\sim 4 - 15$ μm) detectors on-board ISO (PHT-S, CAM, SWS) we have $E_0/E_j >> 1$ while for the Ge:Ga ($\sim 40 - 150$ μm) detectors (PHT-C, LWS, SWS) we have $E_0/E_j \sim 1$ or $<< 1$.

The consequence is that for Ge:Ga detectors the Fouks-Schubert model does not seem appropriate. No accurate analytical models can be derived from the set of equations which describe the problem. Numerical models (Haegel et al. 1999) exist but need big computing resources and are very difficult to compare with data, and they cannot be used like analytical models to do transient corrections.

`TR: Application of Fouks-Schubert transient correction method to point sources in ISOCAM data (September 1999) Alain Coulais`

Concerning the application of Fouks-Schubert method to point sources, several models have been tested. The main problem is how to deal with cross-talk between adjacent pixels to perform the transient correction.

Efforts have concentrated so far on data taken with CAM with the 1.5″ lens and filters LW10 and LW3 (largest PSF) where the lowest spatial gradients on individual pixels are expected.

None of the empirical models tested give correct responses (closer than 10% for each pixel and each readout).

However, quite satisfactory results are obtained when the Fouks-Schubert method is applied not to the individual pixels but to the integrated emission obtained by adding up the contribution of all the individual pixels where signal has been detected from a given point source.

In this case, even when the individual response of the pixels is not monotonous and very noisy, the integrated value of the signal over a typical area of 3x3 pixels centred around the peak of emission was found to be monotonous and smooth.

This means that an alternative to perform accurate photometry of point like sources could be the application of the Fouks-Schubert method not to the individual pixels but to the integrated emission detected from each point source in a CAM field. Some cases have been tested where the mean values obtained after stabilization are well reproduced by the Fouks-Schubert method. Investigations in this direction are on-going (see Figure 20).

`TR: SLICE: a new tool to correct for long-term transients in ISOCAM data (October 1999) - Marc-Antoine Miville-Deschenes`

Long-term transient effects are sometimes observed in CAM observations which are not taken into account in the usual transient corrections. They are the consequence of very slow flux stabilization (few per-cent per hour) and could completely dominate large scale emission. The effect seems to be smaller for small flux steps but the origin is not understood. Long-term transients cannot be predicted and thus no automatic correction is possible.

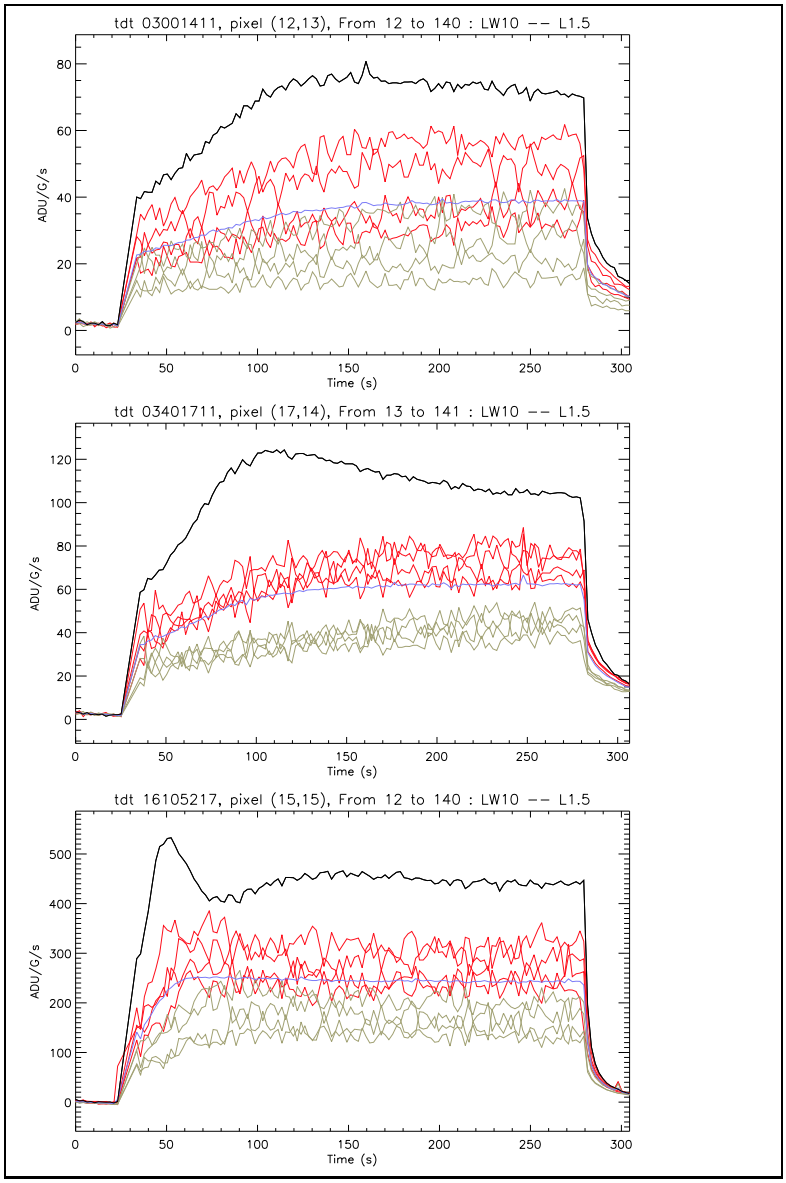

Figure 20: A few examples of signals cøming from the 3x3 pixels around point sources detected with CAM. The central pixel is plotted in dark; in red, the four closest neighbour pixels; in yellow the four pixels in the corner; the blue line is the mean of the 9 pixels. Note that even although the mean value always shows a monotonic behaviour, it cannot be reproduce by the Fouks- Schubert model - Alain Coulais

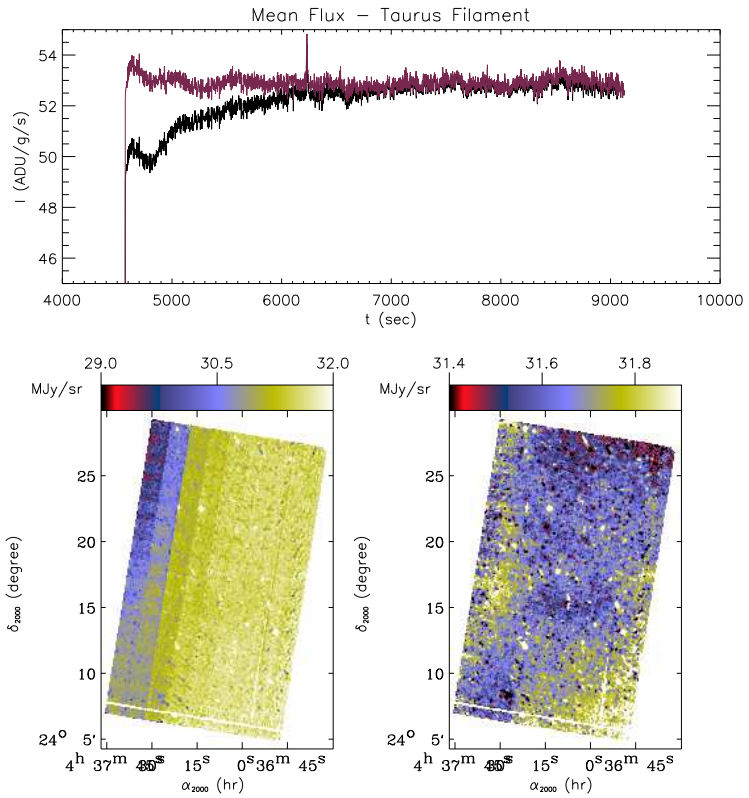

Figure 21: An example of the application of the SLICE S/W package to CAM data. In the upper panel the mean flux is plotted before and after long-term transient correction. The CAM image is displayed below before and after the application of the correction - Marc-Antoine Miville-Deschênes

SLICE is a new software package for long-term drift correction of CAM images developed by Marc-Antoine Miville-Deschênes. Only valid for highly redundant raster maps, it has recently been integrated in CIA (version JUL99), strongly improving the detection limit of faint extended features in the CAM maps of Diffuse Interstellar Clouds where this method has been applied. When variable flat-field effects are corrected the achieved accuracy can be better than 0.1 %. The results are just limited by read-out and photon noise equivalent to 100-200 μJy (see Figure 21).

An alternative for the correction of long-term drifts is the use of analytical models (physical or empirical) like the Fouks hyperbolic model, but the application to real data is difficult and only valid for specific cases.

```
TR: Application of Fouks-Schubert transients correction method to
     LWS data (October 1999)
        Emmanuel Caux
```

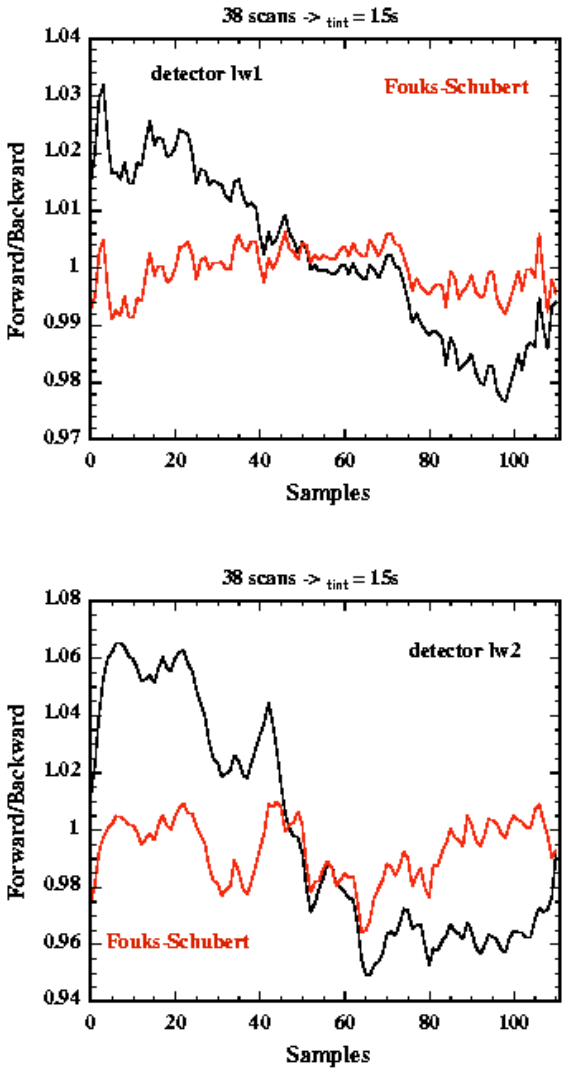

Figure 22: Ratio of LWS forward/backward scans before and after the application of the Fouks-Schubert transient correction - Emmanuel Caux

Emmanuel Caux reported at the last Transients WG meeting on the latest results obtained with an adaptation of the Fouks-Schubert correction method applied to LWS data.

Although the Fouks-Schubert model is in principle not applicable to Ge-based detectors (with the exception may be of LWS parallel mode observations), memory effects can be at least partially removed for LW detectors which are based on Ge:Ga (note that the stronger memory effects are observed in the stressed Ge:Ga detectors LW2 to LW5) by the application of this modified Fouks-Schubert correction method.

Satisfactory results are obtained in all cases with the modified Fouks-Schubert method (see Figure 22). In some cases additional improvement is achieved by applying a correction for overshooting effects sometimes observed in the data for big flux jumps and also available.

The situation is worse for Ge:Be detectors (the case of SW1) where Fouks-Schubert apparently does not work.

The plan is to apply the modified Fouks-Schubert correction method to the LWS RSRFs (at least for LW detectors) and evaluate the impact that the correction for this effect produces on the whole LWS calibration. The improved RSRFs so obtained will be implemented in LIA first, and eventually in the pipeline (probably not before OLPv10).

TR: Report on IFSI activities on LWS transient effects (October 1999) - Stefano Pezzuto

Stefano Pezzuto presented at the last WG meeting a summary of activities developed at IFSI concerning correction of transient effects in LWS data.

A simple approach is used which describes the problem as an autoregressive process. Equations are obtained which correspond to the discrete description of a physical system with 'memory' and a time constant 'T'.

Assuming a spectrum x(i) and a given RSRF, it is straightforward to derive the output signal y(i). The problem is to derive x(i) given y(i).

This inversion has to be made in three steps:
1) the determination of N (the order of the autoregressive process);
2) the determination of the values of the coefficients α_i
3) the correction of the observed spectrum.

The determination of the coefficients α_i need as input a stationary random signal Z (noise).

There are two cases for LWS data in which the input can be considered pure noise:

1) The first case is the signal measured by inactive detectors during an FP observation, but then the noise is given by the electric circuit as a whole and $E[\alpha_1] = 0$.

2) The second case is the signal from a (moderately) strong source with the grating at a fixed position. The signal is then intrinsically stable and fluctuations are dominated by the noise of the detector. In this case the coefficients α_i can be derived.

Future work includes:
1) Analysis of FP observations (it is expected that $\alpha_1 \sim 0$ for the inactive detectors;
2) Analysis of observations with the grating at fixed positions (planets?)
3) Comparison with results from other approaches (Fouks-Schubert theory);
4) Correction of spectra (deconvolution).

TR: Transients correction in PIA/PHT pipeline: revision of status and plans (October 1999) Carlos Gabriel

Carlos Gabriel reported no additional progress in transient corrections of PHT data since the last meeting.

Several transients correction methods are currently implemented in PIA. Drift recognition and exponential fits to data are applied to P3, C100 and C200 detectors (Ge:Ga). A Fouks-Schubert correction is also implemented in IA

that can be applied to P1 and P2 filters (Si-based) and PHT-S measurements. However, the detector specific constants of P1 and P2 filters have not been fully determined and the model cannot reproduce the often appearing hook responses in the signals of these detectors. The only mode for which a broad application of both the full Fouks-Schubert model and the signal jump has been demonstrated is the chopped PHT-S mode. In OLP v8.4 an empirical model is used to correct PHT-S chopped data for transients which is based on the comparison of behaviour with respect to reference stars. A new method based on pattern recognition to be applied both to PHT-S and PHT-C chopped data is currently under development in Heidelberg. For PHT-S staring observations the dynamic calibration method is prefered, which will be implemented into OLPv9.0.

`TR: Analytical solution to the transient problem in SIRTF/MIPS detectors using Burgers' equation (October 1999) Misha Pesenson`

Misha Pesenson presented an analytical description of how non-monotonic transients can be obtained using Burgers' equation (a generalization of the Fouks-Schubert equations when diffusion and non-linear drifts are considered in the detectors).

Non-monotonic transients are expected to be frequent in Ge:Ga detectors like the MIPS/SIRTF detectors and have also been observed in ISO PHT chopped observations.

In the presentation, various existing approaches to correction of transients were reviewed, discussed and compared.

It has been found that Burgers' and Fouks-Schubert's methods agree within 1% in the prediction of the asymptotic value in the case of monotonic transients even when only the initial 30% of the data (before the asymptotic level is reached) is known.

Only by considering the Burger's equation instead of the more simple Fouks-Schubert approach it is possible to produce non-monotonic (hook-shaped) transients like those sometimes observed in the data.

However, there is no algorithm available yet able to identify and recover hook-shaped transients when only a fraction of the data is known before the stabilization level is reached. Efforts are still on-going.

Interactive Analysis

It was only after the issue of the First Status Report that the WG activities reached full strength. The WG has concentrated so far on conducting discussions

via e-mail and during two meetings in the last six months, the last of which was held at VILSPA on November 3, 1999, on the the different Interactive Analysis (IA) software packages available for data reduction.

Questions were addressed like reasons behind design decisions, maintenance strategies or problems derived from the fact that the IAs have to be supported under multiple operative systems or with pieces of code written in different programming languages.

Discussion also concentrated on recommendations to future missions, like FIRST, considering the experience of ISO. Some of these recommendations are summarized here:

- Use the minimum number of programming languages
- Support the minimum number of operative systems
- URD (user requirements) documents must be written by astronomers while ADD (architectural design) documents must be writen by S/W engineers
- Developer teams must be composed both by scientists and S/W engineers
- Calibration observations should be performed as much as possible under the same conditions as science observations (not done in many cases by ISO).

The WG felt that a good access and feedback to the user community is essential when developing S/W. In order to improve the communication flow with the users, the decision was taken by SWS, PHT and LWS members of the WG to follow the initiative of CAM and send an e-mail questionnaire out to users soliciting thoughts on their IAs. These questionnaires will soon be sent out to users.

The implementation status and plans were reviewed by the members of the WG per IA. A summary of the information provided can be found below.

- **PIA v8.0:** (released September 22, 1999)

  - a major step forward in the calibration of ISOPHOT data.

  - signal linearization is fully implemented and must be used, since many calibration files depend on it.

  - a new way of reducing chopped data (*ramp pattern* analysis) is now the default method.

- the use of PSF factors for individual C100 and C200 pixels was introduced. The possibility of flux extraction from maps using them is implemented.

- a new Spectral Response Function for PHT-S chopped measurements, including a first-order correction is now used.

- a filter-to-filter correction for PHT-P measurements is implemented.

- a new bitflag system is in place which makes possible to recognize why data points are flagged, to reset them and/or change the severity criteria.

- the analysis of nodding observations including background subtraction is implemented.

- faster processing (a factor 3–5 better) is achieved through fundamental changes in the SRD derivation.

- the possibility of flux calibrating FCS measurements added.

- a new flat-field correction method (specially suited for mini-maps) introduced.

- intrinsic noise calculations for maps with undefined uncertainties added.

- an interface to IRAF's Drizzling mapping method is implemented.

- **PIA v8.1:** (released November 4, 1999)

  - mainly a fix of a bug in the processing of PHT-S chopped data which made not possible the use of the new calibration method for this type of observations;

  - it also includes a pointing effect correction for PHT-S; a few arcsec off-centre positioning of a point source observed by PHT-S can lead to a significant change both in intensity and spectral shape. The possibility exists of graphically compare corrected versus uncorrected spectra and edit the input parameters.

- **CIA v4.0:** (will be released in December 1999)

  - it contains many new modules for the application of the Fouks-Schubert transient correction method or the Wozniak transient correction

  - the SLICE software package to correct for long-term transients in highly redundant CAM rasters has been integrated (it is now possible to convert a CIA raster to a SLICE data set, process it with SLICE and get it back to CIA). More info on SLICE functionalities will be contained in a SLICE users manual.

- outdated transient corrections are removed.

- a new dark model is used.

- users will be warned of saturations in the data. The position of the saturated pixels can be obtained and masked out.

- it is expected to be Y2K compliant and will make use of IDL 5.2.

- **OSIA v1.0:** (released December 15, 1998)

  - this is the public version of the SWS Interactive Analysis system used in the calibration of the SWS instrument.

  - it basically contains the same routines that are used in the SWS pipeline.

  - OSIA v2.0 will be released after OLP 9.5 (September 2000). The final version 3.0 will be released after OLPv10 (April 2001)

- **LIA v7.3:** (released November 9, 1999)

  - LWS calibration observations of Mars are used to perform the Fabry-Perot throughput correction

  - in the reduction of Fabry-Pérot data the user has the option of displaying the full grating scan data (AOT LWS01, if available) on top of the FP data for the source in question; this is useful to make a more reliable estimate of the dark current and the straylight in the FP data.

  - improving the DC subtraction for a given detector is possible without doing the job all over again.

  - most inspection routines can produce PS plots, using the */hard-copy* keyword on the command line.

- **ISAP v1.6:** (released January 19, 1999)

  - new data reduction recipes are provided for SWS and LWS AOTs

  - the user may read-in and manipulate the Survey Products from the ISO Data Archive

  - the splitting of Auto-Analysis Results into separate data sets has been automated and installed as a special function in the Graphical User Interface.

  - data which has been flagged as bad by the pipeline processing (as glitched data, data following a glitch, saturated fluxes, out-of-detector passband, etc.) may be overplotted on the good data.

  - Shift has an additional mode: LWS dark. It shifts one detector to match an adjacent one using a method that includes knowledge of the LWS RSRF function (as is needed to simulate the adjustment to the dark current removal).

  - data outside the nominal LWS detector bands (which are now provided by OLPv7) may be removed automatically.

- improved average, clipping and inversion routines and documentation.

- a header editor has been implemented.

- a running journal of user-issued commands is kept within the data header.

- ISAP v2.0 will be released in December 1999/January 2000. After December 15, 1999 the code will be frozen and ISAP will go officially into *maintenance mode*.

2.3 Updated overall schedule

Below is the updated schedule for cross-calibration activities in the framework of the important events (impacting instrument calibration) during the remaining POPS. It contains all on-going actions previously identified and reported in the Cross-calibration Plan which are still pending as well as new actions activated during the last six months not previously included in previous versions of the Cross-calibration Plan.

Note that a major change in the new schedule below are the new delivery dates for future OLP releases (versions 9.0, 9.5 and 10.0) only recently agreed by all the parties involved.

A graphic version of this schedule can be found at:

`http://www.iso.vilspa.esa.es/users/expl_lib/ISO/schedule_plan_2.ps`

CROSS-CALIBRATION PLAN

(as of November 25, 1999)

```
================================================================================
        * Second Post-ops X-Cal. Status Report            2 Dec. 1999
             (on OLPv8)
================================================================================
TR: SLICE S/W package for long-term transients correction integrated in
     CIA v4.0 (December 1999)
GL: Characterization of glitch tails: final results (December 1999)
        Ana Heras
PO: ISOPHOT Polarisation: final document (December 1999)
        Ralf Siebenmorgen
PH: Cross-calibration analysis of Neptune observations with SWS, PHT-S
     and CAM-CVF (December 1999)
        Bernhard Schulz
BP: Implementation of LWS conversion factors from point source to extended
```

source fluxes in ISAP 2.0 (December 1999)
LP: LWS line profile stability analysis: extension to a larger number of lines and targets, including dependence on time and scan direction (January 2000)
Rosario Lorente
BP: ISO telescope asymmetric PSF model revision (January 2000)
Koryo Okumura
BP: Ghost correction matrix: revision of status (January 2000)
Koryo Okumura
BP: Implementation of SWS beam profile calibration files in SWS IA (January 2000)
BP: Implementation of SWS pointing correction calibration files in SWS IA (January 2000)
BP: Analysis of a possible synchronization problem between ISO pointing files and recorded data (January 2000)
TR: Implementation of the adapted Fouks-Schubert method to correct SWS band 2 data for transients in SWS IA (January 2000)
Do Kester
PH: Statistical cross-calibration analysis of sources in the ISO Data Archive observed with CAM-CVF, PHT-S and SWS: final results (January 2000)
Pedro Garcia-Lario
LP: Extension of analysis of SWS line profiles to a larger database and implementation of a cross-talk correction (February 2000)
SM: Investigation on discontinuities found between SW1 and SW2 bands in LWS and possible trends with source properties (February 2000)
Alberto Salama
SM: Correction for straylight from Jupiter applied to the LWS spectrum of Callisto (February 2000)
SM: Analysis of spectral line fluxes; comparison with external - KAO - data (February 2000)
Martin Burgdorf
SM: Cross-calibration analysis of SWS, PHT-S and CAM-CVF observations of Neptune (February 2000)
Bernhard Schulz
PH: Statistical cross-calibration analysis of sources in the ISO Data Archive observed with LWS and PHT-C filters (February 2000)
Pedro Garcia-Lario
PH: Workshop "ISO Beyond the Peaks" to be held at VILSPA (February 2-4, 2000)
PH: Correction for non-linearity of detector responsivity for data sets covering a large flux range implemented in OLP v9.0 (February 2000)
PH: Chopped photometry corrections implemented in OLP v9.0 (February 2000)
TR: Implementation of the dynamic calibration method to correct for transients in PHT-S staring observations in OLP v9.0 (February 2000)

==========

$ Delivery of Cal-G files for OLPv9.0 (CAM+PHT) 15 Feb. 2000

==========

* POPS mid-term review 16-17 Feb. 2000

==========

```
IA: Report on recent improvements implemented in the four ISO instruments'
     IAs (March 2000)
PO: CAM polarisation: results obtained with the use of an improved
     de-glitching strategy (March 2000)
       Ralf Siebenmorgen
PO: PHT polarisation: revision of status concerning inconsistencies
     between C200 pixels (March 2000)
       Rene Laureijs + Ulrich Klaas
GL: Glitch statistics: revision of status for all the instruments
      on board ISO (April 2000)
GL: Report on latest results on PACS radiation effects simulations
     (April 2000)
SM: Analysis of spectral line fluxes; comparison between measurements on
     the same line obtained by different ISO instruments (April 2000).
TR: Applicability of transient corrections to point sources: revision of
     status (April 2000)
      Alain Coulais
TR: Improvement of SWS and LWS RSRFs after correction for transient
     effects: evaluation of results obtained (April 2000)
      Do Kester (SWS) and Emmanuel Caux (LWS
TR: Transient effects in SWS band 4 data: revision of status (April 2000)
      Do Kester
TR: Characterization of memory effects affecting Fabry-Perot LWS
     line profiles  (April 2000)
     Anna di Giorgio
TR: Progress report on IFSI activities on LWS transient corrections
      (April 2000)
      Stefano Pezzuto
PH: Evaluation of the effects of pointing correction applied to PHT-S data
     on the photometric accuracy of PHT-S (April 2000)
PH: Statistical cross-calibration analysis of sources observed with SWS and
     LWS and comparison with IRAS data available (April 2000)
      Pedro Garcia-Lario
PH: Evaluation  of calibration improvements recently achieved
     and investigation on cross-calibration problems reported
     in the last Status  Report affecting OLP and/or  IA data
     with special emphasis on IA data products (April 2000)
================================================================================
        * OLP 9.0 (CAM+PHT) IDC --> NDCs                  17 May 2000
================================================================================
        * Third Post-ops X-Cal. Status Report             08 June 2000
              (on IAs cross-calibration)
================================================================================

BP: Implementation of SWS beam profile calibration files in IA and
     OSIA (May 2000)
BP: Implementation of SWS pointing correction calibration files in SIA
     and OSIA (May 2000)
GL: Implementation of improved glitch detection algorithms in SWS
```

```
     OLPv9.5 and OSIA (May 2000)
TR: Implementation of the adapted Fouks-Schubert method to correct SWS
     band 2 data for transients in OLP v9.5 and in OSIA (May 2000)
       Do Kester
BP: Description  of  final  status  of  ISO Pointing reconstruction and
     improvements during post-operations (June 2000)
        Andy Pollock + Alberto Salama
LP: LWS  line  profile stability analyisis:  dependence on detector and
     line strength and deviations from gaussian fit (June 2000)
        Rosario Lorente
PO: ISOCAM Polarisation: final document (June 2000)
        Ralf Siebenmorgen
================================================================================
       * Delivery of Cal-G files for OLPv9.5 (SWS)        15 June 2000
================================================================================
GL: Implementation of improved  de-tailing algorithms in SWS IA (August
     2000).
================================================================================
       * OLP 9.5 (SWS) IDC --> NDCs                     15 September 2000
================================================================================
GL: Implementation of a more sophisticated de-glitching method in PHT
     OLP v10.0 (October 2000)
PH: Correction for inhomogeneous illumination of PHT-P apertures
      by FCS implemented in OLP v10.0 (October 2000)
BP: Beam profile corrections for PHT-P filters data implemented in
      OLP v10.0 (October 2000)
PH: Surface brightness calibration in PHT raster maps available in
      OLP v10.0 (October 2000)
PH: Implementation of refined flat-field corrections in raster maps
     taken through PHT-C filters in OLPv10.0 (October 2000)
TR: Implementation in OLP v10.0 of any not yet implemented transient
      correction currently available in PIA (October 2000)
TR: Implementation of non-linear long-term drift corrections in PHT
      raster maps in OLP v10.0 (October 2000)
PH: Implementation in OLP v10.0 of a new dark subtraction method in SWS
     band 2 data (October 2000)
GL: Implementation of new glitch detection methods and de-glitching
     algorithms in CAM pipeline v10.0 (October 2000)
TR: Implementation of transient corrections in CAM OLP v10.0 applicable to
     point sources (t.b.c.)
      (October 2000)
BP: Implementation of a ghost correction matrix in CAM OLP v10.0
      (t.b.c.) (October 2000)
TR: Implementation of an adapted Fouks-Schubert transients correction
      to LWS data in OLP v10.0 (t.b.c.) (October 2000)
BP: Implementation of beam profile calibration files for LWS data in
      OLP v10.0 (t.b.c.) (October 2000)
GL: Implementation in OLP v10.0 of an improved glitch detection algorithm
     in LWS data (October 2000)
PH: Improved correction of fringes in LWS data implemented in OLP v10.0
```

```
     (October 2000)
PH: Implementation in OLP v10.0 of an improved dark current subtraction
      method in LWS data for faint sources (October 2000)
IA: Report on recent improvements implemented in the four ISO instruments'
     IAs (October 2000)
PH: Evaluation  of calibration improvements recently achieved
     and investigation on cross-calibration problems reported
     in the last Status  Report affecting OLP and/or  IA data
     with  special emphasis on  OLPv9  data products (October
     2000)
================================================================================
       # Freeze calibration algorithms for OLP   01 Oct. 2000
================================================================================
       $ Delivery of CAL_G files for OLPv10 (all)         01 Nov. 2000
================================================================================
       # Working Group Final Reports - drafts -           15 Nov. 2000
================================================================================
       * Fourth Post-ops X-Cal. Status Report             01 Dec. 2000
            (on OLPv9)
================================================================================
PO: Internal cross-calibration of ISO Polarisation measurements
     (December 2000)
================================================================================
       * Official end of ISOSDC at MPE                   31 Dec. 2000
================================================================================
LP: LWS line profile stability analyisis: behaviour of point-like versus
     extended sources (January 2001)
================================================================================
       # Working Group Final Reports             01 Feb. 2001
================================================================================
       * OLP 10.0 final OLP IDC --> NDCs                 09 Feb. 2001
================================================================================
PH: "ISO Calibration Legacy" Workshop to be held at VILSPA (February 2001)
PO: External  cross-calibration of ISO Polarisation measurements
     (March 2001)
IA: Report on recent improvements implemented in the four ISO instruments'
     IAs (March 2001)
PH: Evaluation  of  calibration  improvements recently achieved
     and  investigation on cross-calibration  problems reported
     in the last  Status  Report affecting  OLP and/or  IA data
     with special emphasis on OLPv10 data products (April 2001)
================================================================================
       * Final Post-ops X-Cal. Status Report             01 Apr. 2001
           (on OLP v10)
================================================================================
LP: Comparison of results found both for LWS and SWS with the theoretical
     instrumental profiles and resolution (May 2001)
LP: Line profile definition, recommendations and caveats (May 2001)
PH: Description of photometric data reduction in IA's that couls not be
     implemented into OLP processing due to being appropriate to only a
```

subset of data or to limited OLP implementation resources (May 2001)

* ISO Explanatory Supplement final issue	01 May 2001
* ISO Data Archive final delivery	01 May 2001
* Legacy (final) archive available to community	01 Aug. 2001
* End of ISO NDC at Saclay/Orsay	31 Dec. 2001
* End of ISO NDC at MPIA	31 Dec. 2001
* End of ISO NDC at RAL	31 Dec. 2001
* End of Post-operations Phase	31 Dec. 2001

3 Internal and external cross-calibration

3.1 The concept of cross-calibration

Cross-calibrations can be used (i) as consistency checks, and (ii) as true calibrations. In the first instance observations of a source by a pair of instruments are compared to evaluate internal consistency: if the results do not agree (to within the stated uncertainties) then the calibration procedure of one of the instruments (though possibly both) is incorrect. In the second instance, results from the less accurate instrument(s) are calibrated against data from the more accurate one(s).

In the case of ISO, the above concept can be applied both to pairs of ISO instruments that overlap in wavelength range and also to ISO instruments vs other non-ISO instruments.

3.2 Definition of standard and cross-calibration sources

The absolute flux calibration of three of the four ISO instruments (CAM, PHT and SWS) is based primarily on results of the Ground-Based Preparatory Programme (GBPP, Jourdain de Muizon and Habing, 1992 Les Houches Series: Infrared Astronomy with ISO, p. 129) and of the Cohen, Walker, Witeborn et al. (CWW) absolute calibration programme (Cohen et al. 1992a AJ 104, 1650, 1992b AJ 104, 2030 and 1995 AJ 110, 275), though the long wavelength filters of PHT also use planets and asteroids to cover the bright and intermediate part of their dynamic range. The absolute flux calibration of LWS is currently based on Uranus as primary source.

For cross-calibration purposes a small set of astronomical sources was used in the past. They include a few bright stars (like HR 7310, HR 7341, HR 6436, γ Dra or α Boo), planetary nebulae (NGC 7027 and NGC 6543), galaxies (Mrk 279), asteroids (Cybele, Hygiea) and planets (Neptune) on which most of the cross-calibration comparisons carried out so far have concentrated. For most of them observations exist taken throughout the whole ISO mission with more than one instrument and in many cases covering a wide range of wavelengths.

Note that, because of the limited common dynamic range between the ISO instruments, not all kind of inter-comparisons are possible. Stars are too faint in the long wavelength range of ISO to be used for cross-calibration analysis in the spectral region beyond 100 μm and asteroids and planets have to be used instead. While the results of the CWW and the GBPP programmes, based on stars, are believed to be accurate to $\pm$5% or better and are consistent with one other, the uncertainties in asteroid and planet model spectral energy distributions are larger (10$-$15% level). In the case of asteroids their characterization is additionally complicated by their variability. Thus, the cross-calibration of LWS in the long wavelength range is specially difficult, since the comparison has to

be made against PHT measurements, and the dynamic range overlap between PHT and LWS is limited.

Another important limitation is imposed by the fact that calibration problems do not necessarily affect all the cross-calibration sources in the same way. Thus, some comparisons do not shed any light on the understanding of a given problem if we restrict our analysis to the small sample of objects listed above.

3.3 A new cross-calibration strategy

In order to take into account all the limitations and caveats considered above a new cross-calibration strategy has been activated based on the statistical analysis of large data sets of sources which consider the following aspects:

- First, cross-calibration must be able to ensure proper handling of differences in beam sizes, filter profiles and spectral resolution, as well as the use of differing absolute calibration systems and of different sets of astronomical standard sources.
- Second, the detailed investigation of specific calibration problems requires the selection of dedicated samples of targets - beyond the small list of astronomical sources listed above, used for general calibration purposes throughout the emission - containing a combination of bright/faint, red/blue, point/extended sources so that a complete picture of the impact of an existing problem on ISO data can be obtained or a new progress in data reduction can correctly be evaluated.

Thus, large data sets of sources have been selected from the ISO Data Archive which satisfy the following conditions:

- they have been observed with more than one instrument/configuration at least once during the ISO mission (for internal cross-calibration purposes)
- infrared data from non-ISO instruments exists (for external cross-calibration)
- accurate models exist against which ISO data can be compared (for absolute flux calibration).

A summary of the first results obtained with this new approach is presented in the next subsection.

3.4 Cross-calibration comparisons

In the following, some of the latest results obtained with this new cross-calibration strategy are shown. The results and analysis presented here put special empha-

sis on those cases where substantial progress has been achieved in the last few months and/or to illustrate a problem under investigation.

The internal and external consistency checks are regularly carried out mainly by the Photometric Calibration WG. They concentrate on OLP data products when a new OLP version becomes available and/or on IA data products when a new data reduction tool is available with expected impact on cross-calibration.

Note that, in the cross-calibration comparisons considered below, when they make use of pipeline data products, the analysis is based on files generated with OLPv8.

When a problem/inconsistency was identified, further analysis was carried out using a more detailed data reduction with the corresponding IAs in order to try to understand the problem and determine whether it can be solved with the tools currenly available within the IAs or additional development is needed.

In future reports similar evaluations will be based on:

Issue	Date:	
#3	May 2000:	data processed with IAs and observation of extended sources
#4	November 2000:	OLPv9 data products
#5	May 2001:	OLPv10 data products (final report)

Cross-calibration analysis of sources observed with SWS and LWS

In the previous Status Report we presented the preliminary results of a comparison study carried out by Alberto Salama on sources observed both with SWS and LWS taking the flux at 44 μm as a reference value to evaluate the level of agreement between both instruments.

A total number of 122 common pointings were selected from the ISO Data Archive for which both SWS and LWS measurements were available. A preliminary analysis of the data indicated that 50% of them showed a flux ratio LWS/SWS at 44 μm within 20% from unity, close to the expected internal consistency between SWS and LWS data (see Figure 23).

The discrepant sources in the sample showed ratios in the range 0.7 to 10. In order to investigate more in detail the wide distribution of values observed, a detailed analysis of the nature of the sources in the sample showing discrepant values (consistency worse than 20%) was carried out by Pedro García-Lario.

Ratios between 1.2 and 6 can naturally be explained if they correspond to extended sources. This is because the aperture increases from $20'' \times 38''$ for band 4 in SWS to $71''$ (a factor of 6.1 larger) for band SW1 in LWS. Thus, stronger LWS fluxes are expected from extended sources.

This is the case of most of the H II regions included in the sample. They show ratios in the above range and are identified as extended sources in the literature.

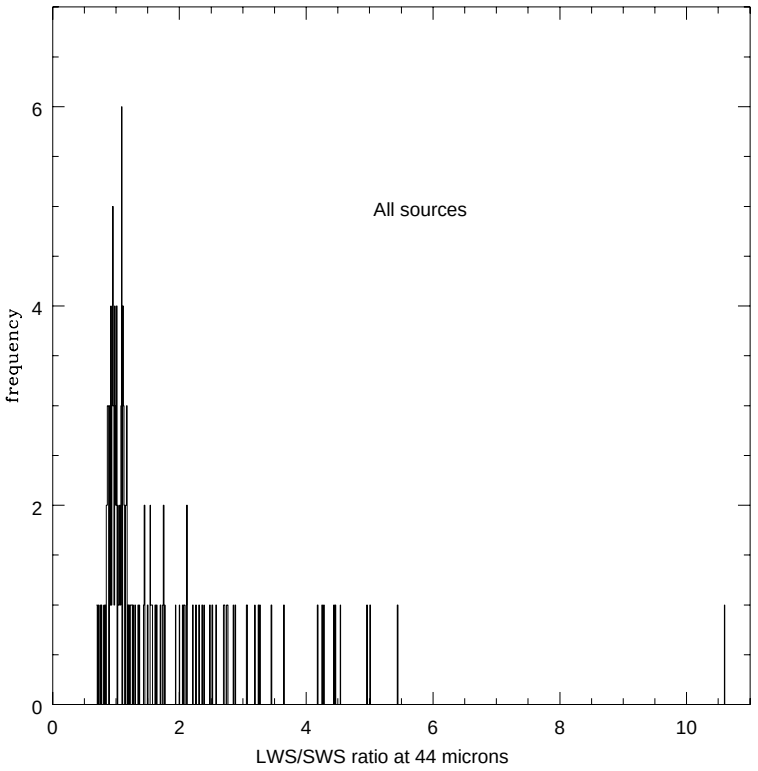

Figure 23: Distribution of LWS/SWS ratios at 44 μm considering all sources in the sample - Pedro García-Lario

In all cases, their extended nature was confirmed through the detection of similar discontinuities between the SWS bands 3D and 3E at 27.5 μm and 3E and 4 at 29 μm (see Figure 24) where the aperture changes from a size of $14'' \times 27''$ (band 3D) to $20'' \times 27''$ (band 3E) and to $20'' \times 33''$ (band 4). Sometimes also jumps are observed betwen bands 2C and 3A at 12 μm where there is also a change in the aperture size.

There was only one case for which a ratio larger than 6 was derived which was found to correspond to a bad-pointed observation of an extended object leading to a strong underestimation of the SWS flux at 44 μm.

In a few additional cases the derived ratio LWS/SWS was below 0.8, below the expected 20% limit of consistency between both instruments. They all turned out to correspond to sources which were identified as strongly variable Mira or OH/IR stars for which the SWS and LWS measurements were not taken simultaneously.

When all the known variable and extended sources in the sample are omitted

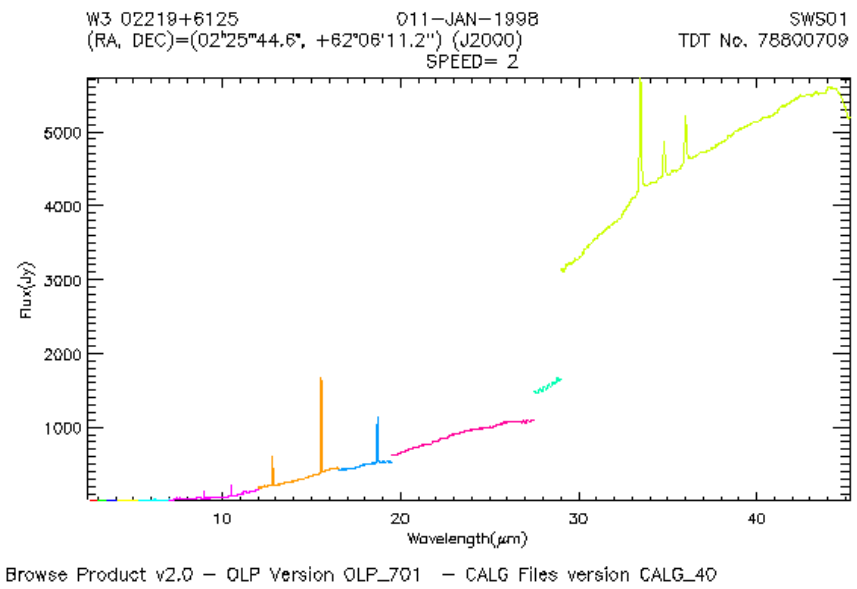

Figure 24: Example of the discontinuities observed in one of the extended sources included in the sample between different bands in the SWS range coincident with changes in the aperture size - Pedro García-Lario

from the level of agreement found between SWS and LWS is within 20(see Figure 25).

Note that an important point to take into account is that the mean value of the LWS/SWS ratios so obtained is <LWS/SWS> = 1.02, very close to unity. This suggests that the Uranus model used for the absolute flux calibration of LWS (in spite of the problems already cited in this document) must be esentially correct, since the band 4 of SWS is calibrated in a totally different way.

Since in several cases objects were repeatedly observed throughout the mission with either SWS or LWS, it was also possible to perform an independent analysis of the reproducibility and stability of both instruments, SWS and LWS. The results obtained indicate that for both LWS and SWS the reproducibility is better than 15% in all cases, although for SWS the number of suitable observations is relatively small to be statistically significant.

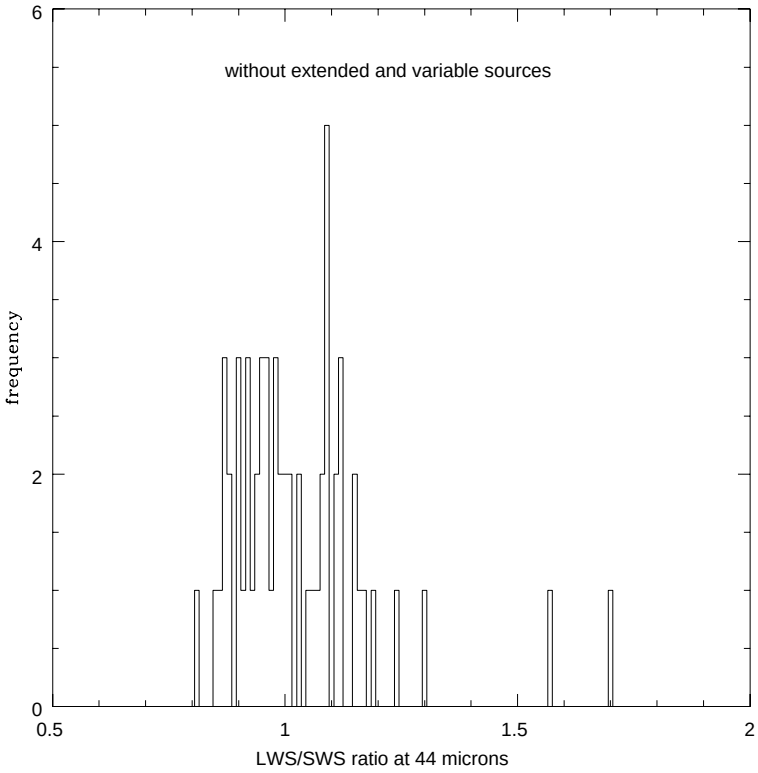

Figure 25: Distribution of LWS/SWS ratios at 44 μm when variable and extended sources are removed from the sample - Pedro García-Lario

Cross-calibration analysis of sources observed with SWS, CAM-CVF and PHT-S

Selection of the sample

A total number of 277 positions in the sky were selected from the ISO Data Archive where spectra have been taken with at least two of the following AOTs: SWS01, CAM04 (CAM-CVF) and PHT40 (PHT-S staring or chopped observations).

Unfortunately, not all the data products retrieved from the Archive are suitable for a cross-calibration comparison. In some cases there are slight pointing offsets which, as we have already mentioned in this document, can account for strong variations in flux. Thus, only pointings which differ by less than $3''$ from

each other were taken into account for the following cross-calibration analysis.

In addition, extended sources have also been excluded from the analysis in this first approach to the problem, since they need of a very careful data reduction as well as the use of aperture size corrections and detailed beam profile models, if what we want is to compare the fluxes measured with the different instruments on board ISO.

Both bad-pointed observations and extended sources will be the subject of independent dedicated analysis in future issues of this Status Report.

If we restrict the analysis to OLP v8 data products corresponding to point-like sources not affected by pointing problems and bright enough to provide reliable data to the analysis, we end up with a database which includes around 20 different sources observed with CAM04, about 200 different objects observed with SWS and a similar number for PHT-S.

Note that the smaller number of CAM-CVF observations is just the natural consequence of the dominant use of this observing mode to observe faint extended sources which otherwise cannot be detected and/or resolved by SWS or PHT. Thus, there is only a small overlap of observations between CAM-CVF and SWS or PHT-S.

SWS versus PHT-S

Starting with the cross-calibration comparison carried out on objects observed both with SWS and PHT-S, Figure 26 shows a few examples of OLP v8 data products corresponding to a few sources in the sample as they were retrieved from the ISO Data Archive, without any additional manipulation.

There is a general good agreement in the overall shape of the spectra in all cases. However, in some cases, strong discrepancies of the order of 20% to 40% are observed in the absolute flux level.

Some of the problems that might be affecting the data in these discrepant cases are well known. They are in a high percentage related with transient effects in PHT-S data taken in staring mode, for which there is still no correction algorithm implemented in the pipeline. This is the case of all the PHT-S observations plotted in Figure 26 with the exception of IRAS 21434+4936 which was obtained in chopping mode and shows an excellent agreement with SWS data already at the OLP level. PHT OLP does not use physical (Fouks-Schubert method) or empirical (exponential, signal jumps) signal transient correction functions for staring observations because they require still a highly interactive mode. Instead, OLP detects transients by statistical trend analysis methods and discards parts of a measurement found to be affected by drifts. This method works well only if a given measure is close to the stability level, which does not always happen.

If this is the case, one should expect to strongly improve the level of agreement of staring PHT-S data with SWS simply by applying the dynamic calibration method to correct the PHT-S data for transient effects using PIA v8.1,

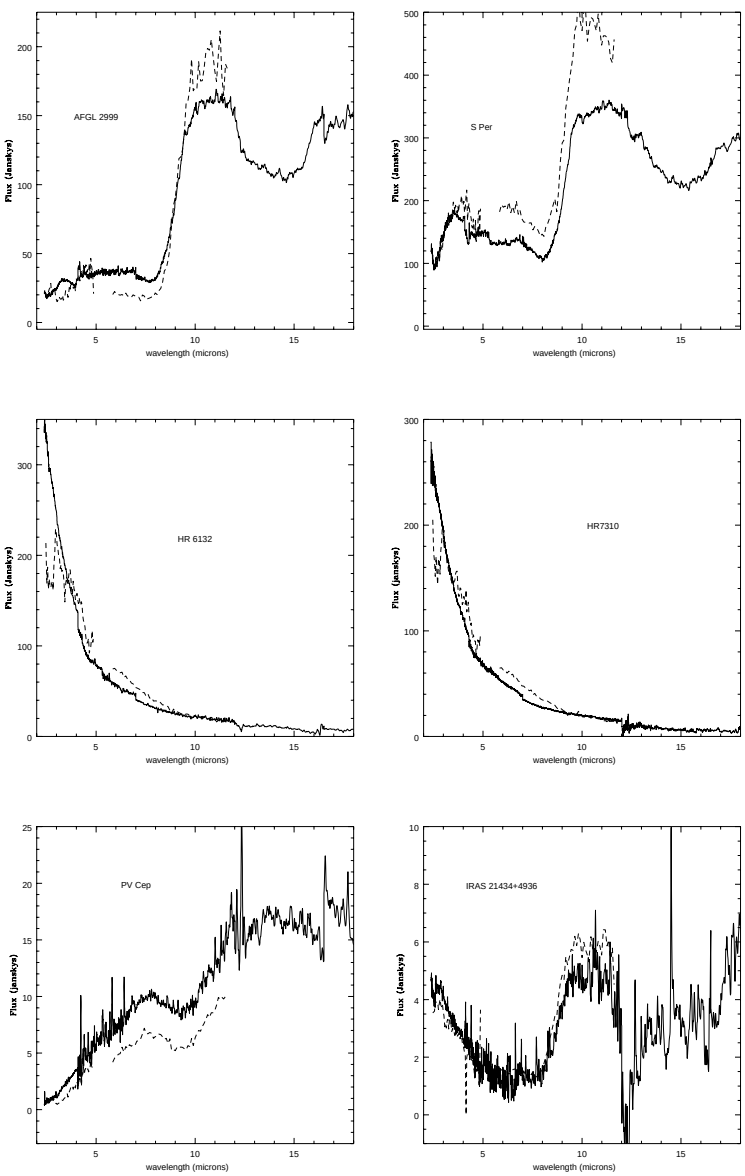

Figure 26: SWS (solid line) versus PHT-S (dashed line) OLP v8 spectra of a few sources in the sample retrieved from the ISO Data Archive

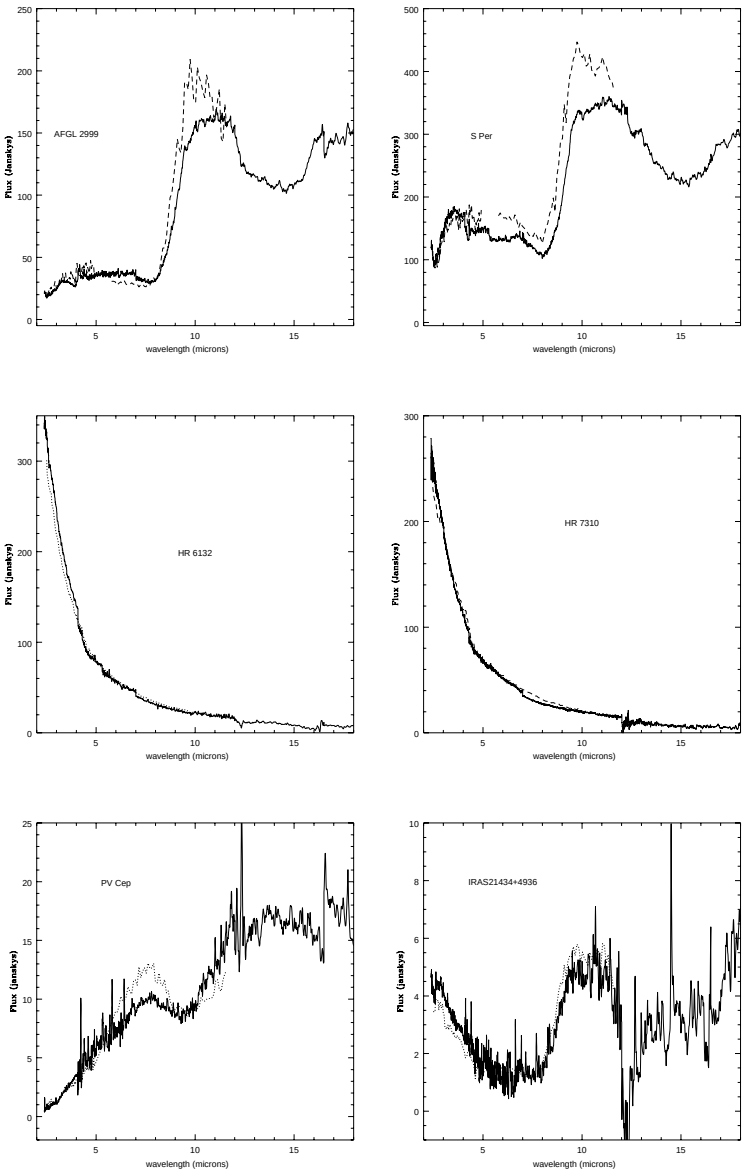

Figure 27: SWS (solid line) OLP v8 data versus PHT-S (dashed line) spectra of the same sources once the PHT-S spectra have been corrected (mainly for transient effects) using PIAv8.1

where several algorithms to correct for this effect are already implemented.

This is what we did and the results obtained after this correction was done are shown in Figure 27 where the same sources were again plotted against the SWS OLPv8 data.

As we can see in Figure 27, the improvement is significant in all cases and the level of agreement reached is found to be better than 5% in some cases, like in HR 6312 and HR 7310.

However, there are still discrepancies which specially affect the brightest sources in the sample, like AFGL 2999 and S Per, at the hightest flux levels. This behaviour will be further investigated.

Note that additional improvements are also expected after the application of the newly adapted Fouks-Schubert transient correction method to SWS band 2 data in all the discrepant cases above cited since it is in the wavelength range corresponding to this band where the agreement observed is worse. Unfortunately, it was not possible to have this correction applied to the SWS data in time before this Status Report was issued.

Smaller discrepancies are also observed in the case of PV Cep, which is a much fainter star, although the agreement between PHT-S and SWS data is also considerably improved after data reduction with PIA v8.1. The strong corrections introduced by the data reduction with PIA suggest that the signal was far from stabilization and this makes the transient correction more difficult. Again, we have to note here that small additional improvements are still expected with the application of transient corrections to SWS band data, still pending.

SWS versus CAM-CVF

Concerning SWS and CAM-CVF cross-calibration comparisons we have plotted in Figure 28 the spectrum of two of the sources in the sample which are representative of the general behaviour observed.

These are the bright star HR 7310 and the fainter star HD 179218. As we can see, there is a general good agreement, within the 15% level, both in the overall shape of the spectra and in the absolute flux level, with the exception of the edges of the CAM-CVF scans, which strongly disagree with SWS data, and some small jumps which look like absorption features in the CAM-CVF spectra. The jump observed in the SWS spectrum of HR 7310 at 12 μm is probably the effect of a bad dark subtraction in band 3A.

A detailed investigation of the CAM-CVF spectra of the two stars above doing manual aperture photometry indicates that the small jumps looking like absorption features in the CAM-CVF data were mainly produced by incorrect

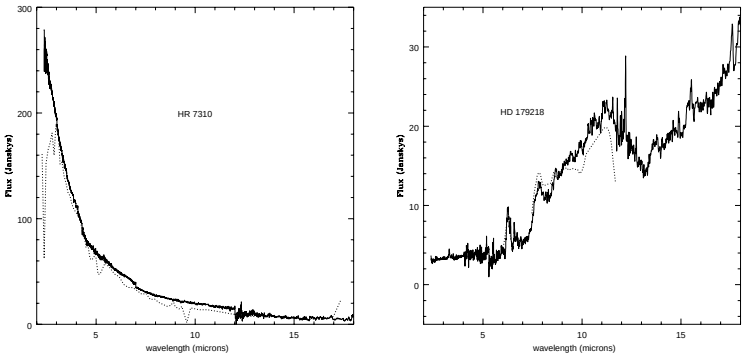

Figure 28: SWS (solid line) versus CAM-CVF (dotted line) OLP v8 spectra retrieved from the ISO Data Archive of two of the sources in the sample

automatic PSF fitting. When the aperture photometry is done manually with the help of CIA v3.0 we obtain a much better agreement with SWS OLP v8 data (see Figure 29).

However, the strong discrepancies observed at the blue and red ends of the CAM-CVF spectrum of HR 7310, due to the effect of transients, for which there is no correction yet implemented in the pipeline, are more difficult to remove.

The currently available transient corrections in CIA v3.0 are in principle only valid for extended sources and the LW range. However, it has recently been shown that a significant improvement can also be obtained if the Fouks-Schubert method is applied to point sources, with the caveat that the method seems to work apparently well only if it is applied not to the individual pixels but to the integrated signal coming from all the pixels where the point source is detected. This correction has not been applied yet to the data shown in Figure 29 and might significantly improve the accuracy of the data. The results obtained after this correction will be presented in a future issue of this Status Report.

Again, we have to remark here that additional improvements are expected in the SWS spectrum after the application of the newly adapted Fouks-Schubert transient correction method to band 2 data, still pending.

CAM-CVF versus PHT-S

In Figure 30 we present the CAM-CVF and PHT-S spectra of two of the sources in the sample which are representative of the general behaviour observed in the cross-calibration analysis of CAM-CVF versus PHT-S data.

Again, we can see that although a general good agreement in overall shape exist, there are in some cases strong discrepancies in the absolute flux level

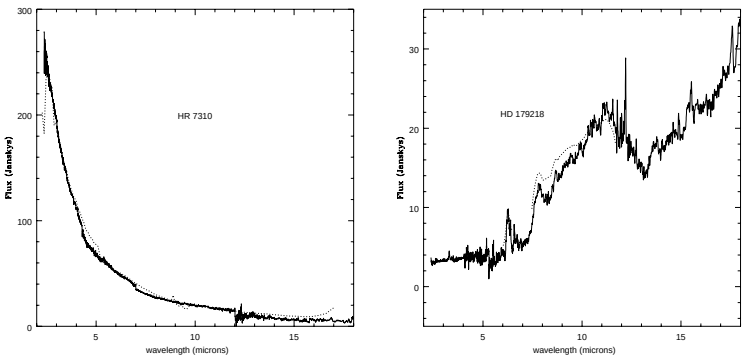

Figure 29: SWS (solid line) OLP v8 data versus CAM-CVF (dotted line) spectra of the same sources once the CAM-CVF spectra have been corrected (mainly for a bad automatic PSF fitting) with manual aperture photometry

which can reach more than 20% in certain regions of the spectral range.

The discrepancies are partially removed when both manual aperture photometry is applied to CAM-CVF data using CIA v3.0 and transients are corrected in PHT-S data using the dynamic calibration method for PHT-S staring observations (see Figure 31).

The results obtained after detailed data reduction are excellent in the case of HR 7310 in the overlapping region between PHT-S and CAM-CVF, where there is almost a perfect match. Again, however, note the incorrect shape of the CAM-CVF spectrum at the blue and red ends due to the transients (correction still pending).

With respect to HD 207129 the situation is worse. Although the shape of the PHT-S spectrum strongly improves after the data reduction with PIA v8.1 note that there is still a relatively strong discrepancy (more than a 20%) with CAM-CVF in the overlapping spectral region which we interpret as due to an overcorrection for transients in the PHT-S spectrum which leads to an overestimation of the flux level. This effect has also been detected in other relatively faint sources where the stabilization of the signal takes always a longer time and the transient correction needed is very strong.

SWS versus CAM-CVF versus PHT-S

Observations are available from the three instruments for a few sources in the sample. This is the case, for instance, of HR 5999, which is taken here as a representative case of how a bit of additional IA data reduction can significantly improve the OLP v8 data currently available in the ISO Data Archive.

Figure 32 shows at the same time the SWS, PHT-S and CAM-CVF OLP

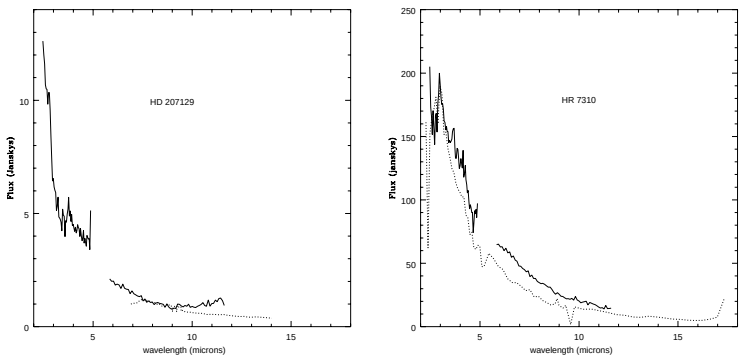

Figure 30: CAM-CVF (dotted line) versus PHT-S (solid line) OLP v8 spectra of two of the sources in the sample as they were retrieved from the ISO Data Archive

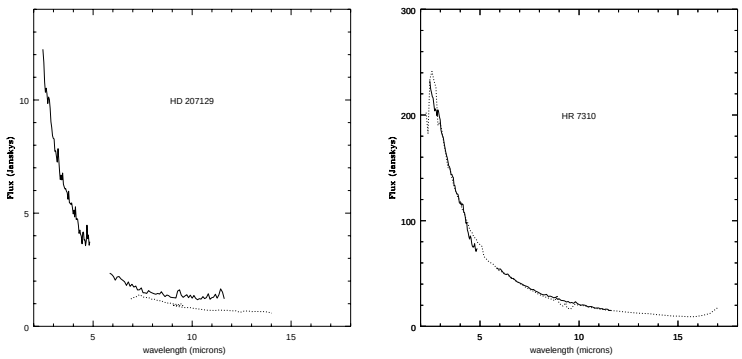

Figure 31: CAM-CVF (dotted line) versus PHT-S (solid line) spectra of the same sources after detailed data reduction with manual aperture photometry for CAM data and PIA v8.1

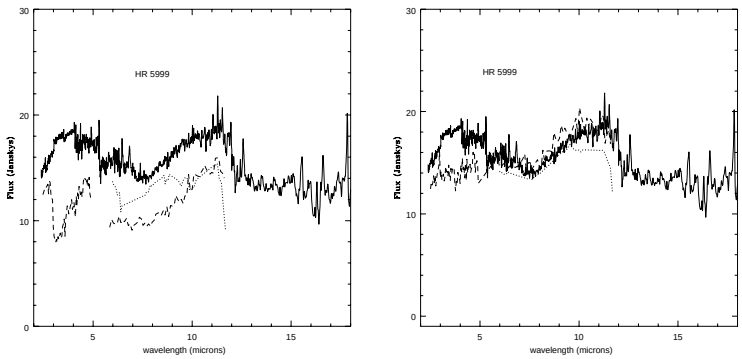

Figure 32: SWS (solid line), CAM-CVF (dotted line) and PHT-S (dashed line) OLP v8 spectra of HR 5999, one of the sources in the sample observed with the three AOTs under analysis, as they are retrieved from the ISO Data Archive (left) and after detailed data reduction with manual aperture photometry for CAM data and PIA v8.1 (right).

v8 spectra of HR 5999 (left) as they are retrieved from the ISO Data Archive together with the results obtained after detailed data reduction with PIA v8.1 and the use of manual aperture photometry for CAM data – SWS correction not yet available – (right).

As we can clearly see in Figure 32, strong transient effects are observed in the PHT-S OLP v8 data specially at short wavelengths which significantly affect the shape of the spectrum. In addition, strong transient effects are also observed in the CAM-CVF spectrum specially at the red end of the spectrum. Finally, the absolute flux level is discrepant in both cases with SWS in more than a 20%.

After detailed data reduction of PHT-S with PIA v8.1 and doing manual aperture photometry for CAM-CVF data using CIA v3.0 a strong improvement in the agreement between the three different instruments is observed. There is a significant increase in flux for PHT-S data after transient correction which brings it into the same flux level as SWS. The shape looks also much closer to SWS at short wavelengths after transients correction. A similar increase in absolute flux level is observed in CAM-CVF data mostly due to the manual aperture photometry. Still, however, the transient effect is observed at the red end of the spectrum and not corrected.

The discrepancy observed at short wavelengths between PHT-S and SWS needs to be further checked against SWS corrected data (still pending) but in general we can conclude that both the overall shape and absolute flux level show a reasonable agreement in most of the overlapping wavelength range between the three instruments after a minimum additional data reduction using the IAs.

4 Calibration accuracies and 'Error Budget'

4.1 PHT

4.1.1 Improvements in OLPv8.4 for PHT

In August 1999 a new version of the PHT OLP (pipeline) for automatic data reduction was released to be part of the new *"On the Fly Reprocessing"*. Note that this means that when PHT data is retrieved from the ISO Data Archive and the *'Latest Processing'* button is selected the user gets the data processed with OLPv8.4.

Version 8.4 of the pipeline represents a major upgrade in the calibration of PHT data. Unfortunately, not all the improvements that are currently available within PIA were installed in this new version of the pipeline and some of them will have to wait until a later version (probably OLPv10 in most cases).

This is a summary of the improvements implemented in version 8.4 of the pipeline:

- **Flux dependent signal linearization:** calibration measurements on celestial standards demonstrate that the detector has a non-linear response. Data used to calibrate the internal radiation sources (FCS) with celestial standards become now more consistent after linearization. Since it is applied early in the signal processing chain, it required the redetermination of several Cal-G files. Considerable changes of photometric results are expected in cases where the FCS measurement is not taken at an adequate power level, like in multi-filter AOTs on targets with a steep spectrum, extended sources - when moving from a small aperture to a large one can easily give a factor of 10 increase in power on the detector (note that the FCS is always tuned according to the brightest flux) - or maps with a high dynamic range.

- **PSF factors for PHT-C arrays** (see *Beam Profile WG* Section): the upgraded PSF factors for the PHT-C arrays provide consistent photometric results, in particular for all filters in C200

- **Multi-filter staring modes:** The OLP processing of the PHT staring modes PHT03 and PHT22 were successfully re-validated. This includes extended source photometry with PHT-C (PHT22). In general, both the absolute and relative calibration are improved by this OLP version.

- **Absolute photometric modes:** The OLP processing of the PHT absolute photometric modes PHT05 and PHT25 were also successfully revalidated. Spectral shapes and features are maintained. Good matches in absolute level and relative shape with reference spectra and photometry are found.

- **Spectroscopy in staring mode on extended sources:** The OLP processing of the spectroscopic mode PHT40 (PHT-S) staring on extended

sources was successfully re-validated. It now contains the updated solid angle determination.

- **Chopped modes:** a new calibration method developed at MPIA was implemented in the pipeline which provides better robustness against glitches and a better correction for the signal losses. It makes use of the periodicity of the measurements and constructs a characteristic pattern, representing both signal levels - on source and off source - by 8 data points. Three classes of patterns were already distinguished: a linear case, a curved case and an overshooting case.

4.1.2 Current calibration accuracies and 'Error Budget' for PHT

The latest report concerning updated PHT calibration status is contained in the document *Release Note for ISOPHOT OLP Version 8.4* by Ulrich Klaas and Phil Richards available at:

`http://www.iso.vilspa.esa.es/users/expl_lib/PHT/olp_84release.ps.gz`

More general information on the calibration status of PHT can be found in the document *ISOPHOT Calibration Accuracies* by U. Klaas et al. available at:

`http://www.iso.vilspa.esa.es/users/expl_lib/PHT/calacc_v3.ps.gz`

Table 1: Covered wavelength range and typical aperture sizes of ISOPHOT subinstruments. Note that for PHT–C the first aperture number denotes the pixel size, the second one the array size.

subinstrument	**detector**	**dimension**	**wavelength range** [μm]	**typical aperture size** ["]
PHT–P	P1	1	3 – 17	5 – 180
	P2	1	15 – 29	23 – 180
	P3	1	40 – 130	52 – 180
PHT–C	C100	3x3	40 – 130	43.5 / 138
	C200	2x2	100 – 240	89.4 / 182
PHT–S	SS	1x64	2.5 – 4.8	24
	SL	1x64	5.8 – 11.8	24

Table 2 gives a summary overview of the currently achieved photometric accuracies. Absolute and relative accuracies as well as relative flux reproducibility are based on the analysis made with OLPv8.4 data products.

Note that a number of AOTs are not yet scientifically validated (see Table 3) and, thus, no global accuracies can be provided. In addition, the two polarisation modes PHT50 (PHT-P) and PHT51 (PHT-C) are processed by the pipeline

Table 2: ISOPHOT Photometric Calibration Accuracy Overview.

detector	**source type** **p**oint / **e**xtended	**source brightness**	**typical on-source integration** [s]	**absolute accuracy** [%]	**reproducibility 1 σ of 20 samples** [%]	**multi-filter accuracy** [%]
P1	p, staring	50 – 6000 Jy	32	< 10	5	< 20
P1	p, staring	0.1 – 50 Jy	≤ 256	40	10	–
P2	p, staring	10 – 200 Jy	32	< 15	2	5
P2	p, staring	0.5 – 10 Jy	≤ 256	< 15	12	–
P3	p, staring	0.5 – 25 Jy	32	10	7	< 10
P3	p, staring	< 0.5 Jy	≤ 256	20	7	–
C100	p, staring	0.5 – 25 Jy	32	15	≥ 3	< 25
C100	p, staring	< 0.5 Jy	≤ 256	40	20	–
C100	e, staring	5 – 15 MJy sr^{-1}	32	25	10	20
C200	p, staring	1 – 900 Jy	128	10	10	< 30
C200	p, staring	0.5 – 1 Jy	≤ 256	< 30	10	–
C200	e, staring	4 – 10 MJy sr^{-1}	64	20	6	20
SS	p, staring	2 – 5000 Jy	256	< 30	< 30	< 30
SS	p, chopped	0.5 – 500 Jy	1024	< 10	–	< 10
SS	e, staring	50 – 10^5 MJy sr^{-1}	256	< 30	< 30	< 30
SL	p, staring	1 – 5000 Jy	256	< 30	< 30	< 30
SL	p, chopped	0.2 – 200 Jy	1024	< 10	–	< 10
SL	e, staring	50 – 10^5 MJy sr^{-1}	256	< 30	< 30	< 30

only to raw data level and are not here considered. It is the goal of ISO Post Operations to scientifically validate the OLP processing of all standard AOTs in Table 3 for which this is pending.

4.1.3 Future plans in PHT calibration

A rough schedule of improvements which will be implemented in upcoming versions of the pipeline is given in Table 3.

Most of the problems above listed are among the list of currently known limitations and caveats which are discussed in Chapter 2 of the *Release Note for ISOPHOT OLP Version 8.4* above cited. The reader is refered to this document for a more detailed description of each of these individual problems.

Note that a careful interactive analysis using PIA may significantly improve the calibration accuracy numbers given above. Unfortunately, it is not possible here to give numbers as a function of the AOT and/or the characteristics of the source observed since so far no comprehensive systematic investigation was performed. But one can expect to achieve a higher accuracy using PIA in the following cases:

Table 3: Status of scientific validation of PHT OLP AOT processing as of version 8.4.

AOT	**observation type**	**submode**	**scientifically valid since**	**next upgrades**	**foreseen in OLP Vx.y**
PHT03 (P)	multi-filter photometry	staring point source	V6	FCS aper	9.0
		staring ext. source	no	beam	9.0
		nodding	V6	FCS aper	9.0
		chopped point source	TBD	chop	8.4
		raster map	no	map cal	9.0
				drift	10.0
PHT04 (P)	multi-aperture photometry	staring point source	no	beam & FCS aper	9.0
		staring ext. source	no	beam	9.0
		chopped point source	no	chop & beam	9.0
PHT05 (P)	absolute photometry	staring point source	V6	FCS aper	9.0
		staring ext. source	no	beam	9.0
PHT17 (P) 18 , 19	sparse map photometry	staring point source	V6	FCS aper	9.0
		staring ext. source	no	beam	9.0
PHT22 (C)	multi-filter photometry	staring point source	V7		
		staring ext. source	V7		
		nodding	V7		
		chopped point source	TBD	chop	8.4
		raster map	V8.4(TBC)	map c al	8.4
				flat-field	9.0
PHT25 (C)	absolute photometry	staring point source	V7		
		staring ext. source	V7		
PHT32 (C)	oversampled mapping	chopped mapping	no	chop & map cal	10.0
PHT37 (C) 38 , 39	sparse map photometry	staring point source	V7		
		staring ext. source	V7		
PHT40 (S)	spectroscopy	staring point source	V5	dyn cal	9.0
		staring ext. source	V6	dyn cal	9.0
		chopped point source	V6		
PHT50 (P)	aperture polarimetry	staring point & ext. source	V7	interactive processing & special FORTRAN routine	
PHT51 (C)	array polarimetry	staring point & ext. source	V7	interactive processing & special FORTRAN routine	
		raster	V7		

meaning of calibration upgrades:

FCS aper : correction for inhomogeneous illumination of PHT-P apertures by FCS
beam : beam profile corrections
chop : chopped photometry corrections
map cal : surface brightness calibration in maps
drift : correction of non-linear long-term drifts
flat-field : refined flat-field corrections
dyn cal :dymamic calibration method to correct for signal transients

1) measurements with signal transients which do not stabilise during the measurement time, but which are long enough to perform a reasonable transient fit.

2) flat-fielding of maps, depending on the sampling mode and the dynamic range.

3) correction of non-linear signal drifts in maps.

4) detection of faint sources by refined deglitching and filtering.

4.2 SWS

4.2.1 Improvements in OLPv8.4 for SWS

In August 1999 a new version of the SWS OLP (pipeline) for automatic data reduction was released to be part of the new *"On the Fly Reprocessing"* system. Note that this means that when SWS data is retrieved from the ISO Data Archive and the *'Latest Processing'* button is selected the user gets the data processed with OLPv8.4.

Improvements in the data reduction over OLP 7 are:

- **Wavelength accuracy improved:** During the mission it was discovered that the relation between the measured position of the grating (called LVDT) and the wavelength was shifting steadily at a rate of about 1 LVDT per 6 months at most. This was corrected by re-deriving the relation every so often. As the shift itself was steady, this procedure resulted in a very low amplitude sawtooth-like behaviour of the wavelength calibration in time. In OLP 8.4 a linear interpolation has been implemented to remove this saw-tooth. The wavelengths are now steady to well within one LVDT, which corresponds to a fraction of a resolution element. The main source of error in the wavelength is (as it was before) the pointing error, corresponding to a few LVDTs.

- **Error information:** Two spare bytes in the AAR product (file swaa*.fits) are used to code the errors on the flux values, which are now used such that byte 0 contains the error in the offset of the slope, in Jy, (from dark current subtraction) whereas byte 1 contains the gain error as a percentage (from the fitting of the ramps themselves). These can be used to generate the 1σ error limits on the spectrum.

- **SPDs and off-band data:** The SPD and AAR products of OLP 7 only contained data from a wavelength within one of the several SWS bands, each band defined by a detector/aperture/order combination - for a list of these bands see Table 3.1 of the *SWS Instrument and Data Manual*. The calibration of data taken outside these bands was not guaranteed. In OLP 8.4, off-band data (i.e. data coming from outside these bands) will be present in the SPD product. This is because it is sometimes useful

to have an overlap region between bands when comparing data. This off band data will not be propagated through to the AAR product. Note that the next release of OSIA, version 2.0, will support off band data.

- **Post-Helium observations:** S95, S96 and S97 are now processed to SPD level and are present in the archive. The wavelength calibration for these observations, however, is not done correctly and care should be taken if they are retrieved from the archive. Contact ISO helpdesk for further information.

4.2.2 Current calibration accuracies and 'Error Budget' for SWS

A document describing the *SWS Calibration Status* as of March 1999, esentially still valid for OLP v8.4 data products is available at:

`http://www.iso.vilspa.esa.es/users/expl_lib/SWS/SWS_Cal_Accuracy.html`

For SWS the goals originally set before the mission (an accuracy of 30% or better) have, in general, been achieved for well-behaved data sets. By well-behaved data sets we understand point sources in the several hundred to several thousand Jansky flux density range that were observed with correct pointing and suffered no instrumental or operational problems.

In Table 4 an overview of flux calibration accuracies of SWS OLP products is given as a function of the SWS band considered. The quoted 'worst' uncertainties are primarily valid for the edges of the bands, representing the maximum product of the absolute and relative spectral responsivity uncertainties. The accuracies given here were determined in June 1997 for version 6 of the pipeline.

The flux reproducibility was checked during the mission by regular observations of the calibration star HR6705. The various measurements agreed to within 6% for band 1 and 2 to 15% for bands 2 to 4.

Unfortunately, an 'error-recipe' for the combination of all the known individual error contributions to a useful overall error estimate for SWS data products does not exist yet.

The problem is that the relevance of the various error contributions depends strongly on the properties of the observed source as well as on the type of scientific analysis that is aimed for.

Thus, no 'error budget' in the true sense can be given, although it is possible to provide the user with an indication of the currently known error contributors.

Some of the known sources of error are:

Detector memory effects: Band 2 (Si:Ga) and band 4 (Ge:Be) are specially affected. Currently, a correction for these effects is not yet available although a transient correction based on the Fouks-Schubert model applicable to band 2 data will be implemented the SWS IA soon and in future versions of the pipeline and OSIA later. The signature of memory effects is that the up- and down-scans are different in flux level. The down-scan normally succeeds the up-scan in the AOT and appears to be already 'accustomed' to the flux level.

Table 4: Overview of the SWS bands and flux calibration accuracy

	Band	Key wavel. μm	Grating order	Aperture number/area "	Detector type	Detector pixels	Wavelength range μm	Accuracy key - worst
SW	1A	2.48	SW4	1 / 14x20	InSb	1 - 12	2.38 - 2.60	5% - 7%
	1B	2.87	SW3	1 / 14x20	InSb	1 - 12	2.60 - 3.02	5% - 7%
	1D	3.08	SW3	2 / 14x20	InSb	1 - 12	3.02 - 3.52	5% - 7%
	1E	3.80	SW2	2 / 14x20	InSb	1 - 12	3.52 - 4.08	5% - 7%
	2A	4.50	SW2	2 / 14x20	Si:Ga	1 - 12	4.08 - 5.30	7% - 12%
	2B	5.90	SW1	2 / 14x20	Si:Ga	1 - 12	5.30 - 7.0	7% - 15%
	2C	7.70	SW1	3 / 14x20	Si:Ga	1 - 12	7.0 - 12.0	11% - 25%
LW	3A	14.0	LW2	1 / 14x27	Si:Ga	1 - 12	12.0 - 16.5	11% - 25%
	3C	17.0	LW2	2 / 14x27	Si:Ga	1 - 12	16.5 - 19.5	11% - 20%
	3D	24.0	LW1	2 / 14x27	Si:Ga	1 - 12	19.5 - 27.5	12% - 20%
	3E	28.5	LW1	3 / 20x27	Si:Ga	1 - 12	27.5 - 29.0	20% - 30%
	4	32.0	LW1	3 / 20x33	Ge:Be	1 - 12	29.0 - 45.2	30% - 35%
	5A	11.8	LW3	1 / 10x39	Si:Sb	1 - 2	11.4 - 12.2	11% - 25%
	5B	14.8	LW2	1 / 10x39	Si:Sb	1 - 2	12.2 - 16.0	11% - 20%
	5C	17.0	LW2	2 / 10x39	Si:Sb	1 - 2	16.0 - 19.0	11% - 20%
	5D	24.0	LW1	2 / 10x39	Si:Sb	1 - 2	19.0 - 26.0	12% - 30%
	6	27.0	LW1	3 / 17x40	Ge:Be	1 - 2	26.0 - 44.5	30% - 35%

Thus, one procedure that has been used to improved data affected by memory effects is to take the down-scan as the reference for the flux level.

Dark current problems: dark currents corrupted by memory effects or glitches usually result also in systematic differences between the up- and down-scans. For large errors in the subtracted dark current, the final spectra will resemble the spectral responsivity. Unfortunately, small dark current problems and memory effects have a similar signature in the final spectra.

Fringes: Bands 2 and 3 can be affected. The amplitude and frequency of the fringes depend on the source morphology, brightness and position in the SWS entrance aperture. Fringe amplitudes of about 5% of the continuum level are seen in band 2 and up to 20% in band 3. Fourier filtering or sine fitting can be used to remove the fringes 'manually'.

Pointing Offsets: As a consequence of the non-uniformity of the detector material and small internal misalignments, the signals in the different AOT bands are reduced by band-dependent factors when a point source is observed with a pointing offset with respect to the centre of the SWS aperture. Corrections for this effect will soon be possible now that the detailed beam profiles have been determined and the actual satellite pointing is known with sufficient accuracy. Pointing offsets are recognized by jumps in the continuum level at band edges in AOTs 1 and 6. In AOT 2 data the effect is very difficult to see.

Glitches: All SWS detector data suffer from cosmic ray hits. Some of them are removed automatically, but especially in the long wavelength bands the removal is far from complete. Tails following a cosmic ray hit are usual in

these bands. Currently, they can only be removed manually within OSIA.

Extended sources: SWS calibration is based on point source emission. As a result, the fluxes derived are not appropriate for extended sources (partially) filling the SWS aperture. At the band edges, jumps in the signal level are seen, which are due to changes in the effective size of the detectors. To obtain reliable flux densities for extended sources, the SWS detector beam profiles should be convolved with the source structure at the appropriate wavelength. As a first order correction, the ratio of the aperture sizes can be taken.

Very weak sources: For very weak sources careful inspection of the data is required to be able to filter out data affected by glitches and determine the true dark current level, while fringes are normally insignificant. Proper calibration and analysis of such data is only possible with much manual labour.

Very bright sources: Very bright sources suffer mainly from memory effects and fringes. The data may also be affected by detector saturation which starts to become important at the several 10000 Jy level. Again, manual labour is needed to deal with such observations.

Generally, for well-behaved data sets, the use of OSIA's tools does not lead to strong improvements in the calibration with the exception of data affected by the presence of interference fringes in band 3 and, to a lesser degree, in band 2.

The situation will change when the improvements listed in the previous subsection will be available in OSIA v2.0, but this will have to wait until mid 2000.

For data sets that are not well-behaved the quoted accuracies are not reached with standard OLP processing. However, often manual processing using OSIA tools allow to reach the same level of accuracy.

4.2.3 Future plans in SWS calibration

Some improvements are hoped to be achieved during the remaining post mission phase with respect to the calibration accuracy of SWS. They include improvements in the determination of the Relative Spectral Response Function and the characterisation of detector memory effects and of the beam profile.

A better understanding of the memory effects will lead to higher accuracies in band 2 and band 4 flux calibration scale (see recent achievements in the *Transients WG* section). In the area of extended sources and bad-pointed observations, a significant improvement is expected once the new SWS beam profile calibration files will be implemented in the SWS IA and eventually in the pipeline (see *Beam Profiles WG* section).

There are plans in the future to update or add a large list of modules to the SWS pipeline processing. They are related to improvementes in: reset cutout length, derive pulse-shape, de-biasing in band 4, AC correction, glitch treatment (including a higher order polynome fit in the glitch detection algorithm, the extension of the search to the full reset interval and the use of a fit slope+step function) and cross-talk corrections.

Unfortunately, most likely not all them will be integrated in OLP 9, but much of it might go only for OLP 10. All these changes will basically lead to a better linearization of SWS integration ramps.

Band 2 transients correction will soon be available. In addition, new RSRFs, corrected for memory effects will be produced and used for data reduction of SWS band 2 data.

Finally, a new dark subtraction method in band 2 completely different to the existing one will have to wait until v10.0 of the pipeline.

It is obvious that the quality of all these improvements can only be judged at the time they are implemented.

4.3 CAM

4.3.1 Improvements in OLPv8.0 for CAM

Version 8 of CAM pipeline is part of the new *"On the Fly Reprocessing"* system since May 1999. Note that this means that when CAM data is retrieved from the ISO Data Archive and the *'Latest Processing'* button is selected the user gets the data processed with OLPv8.0.

This new version contains two changes which may have implications for the science data provided to the user.

- Improved LW *"Optical Flats"* in the Cal-G files.
- Improved non-illumination masking (algorithm to detect non-illuminated pixels at the edges of the array, caused by imperfections in instrument wheel positioning).

Appart from these, no other major changes have been implemented in this new version of the pipeline.

4.3.2 Current calibration accuracies and 'Error Budget' for CAM

The majority of the calibration efforts have concentrated in the last six months on improving the data reduction of CAM data within CIA (see the *Interactive Analysis WG* subsection).

Thus, for pipeline data products the calibration accuracy status of the instrument and the error budget has not changed significantly since the last Status Report.

The latest report on CAM accuracy is contained in the *ISOCAM Calibration Accuracies Document* by Joris Blommaert and Diego Cesarsky (November 1998) which refers to OLP v7 data products and is available at:

`http://www.iso.vilspa.esa.es/manuals/CAM/accuracies/cam_accur/`

An overview of the flux accuracy of the different CAM OLP data products is given in Table 5 for two different brightness levels. The numbers in this Table are based on the analysis of standard stars observed in the central part of the

array. Note that although polarisation observations (CAM05) are handled by the latest versions of the pipeline, the corresponding observing mode has not formally been released yet.

A description of the known sources of error affecting CAM calibration and the corresponding 'error budget' is contained in *The ISOCAM Calibration Error Budget Report* by Andrea Biviano (November 1998), available at:

`http://www.iso.vilspa.esa.es/users/expl_lib/CAM/errdoc.ps.gz`

The following sources of error are identified:

- **Transients:** in general, the dominant error source in CAM images are transients, for which no correction is still implemented in the pipeline. Thus, the use of CIA routines is always needed if we want to improve the accuracy of CAM data affected by transients. In particular, most of the CVF observations are usually performed after a discrete filter observation, thus implying a large decrease in the incident flux on the detector. This can introduce important transient effects that last several readouts and hence several wavelength steps. The result is a larger than true flux for the first wavelength steps. We also know that transients are more important for weak sources than for bright sources and this is the most important reason for the differences in the uncertainties quoted in Table 6.

- **Glitches:** the contribution of glitches to the overall noise of CAM inages is also important. 'Common' glitches are associated to impacts of cosmic ray electrons while the so-called 'faders' and 'dippers' are linked to impact of protons or α particles. Tipically, 'common' glitches are easy to remove while the rare 'faders', followed by a slow decrease of the signal, and 'dippers', followed by a reduction in the sensitivity of the affected pixel, have a long lasting effect more difficult to remove. Unfortunately, since the detection of glitches in the pipeline is based on simple median filtering algorithms, only a fraction of them are automatically removed and manual processing with CIA is needed.

- **Point Spread Function:** the fluxes for point sources in the CPSL (CAM Point Source List) FITS file are derived by PSF-fitting in the image. This photometry can be affected by larger errors than stated in Table 5 if

Table 5: ISOCAM Photometric Calibration Accuracy Overview.

CAM AOT	> 100 mJy key	> 100 mJy worst	<100 mJy
CAM01	10%	20%	30%
CAM03	10%	20%	30%
CAM04	15%	40%	40%
CAM05	-	-	-

the fitting is incorrect. The observed PSF is generally quite close to the theoretical one if the ghost contribution is not significant (see below). However, the accuracy of the PSF does not allow deconvolution yet.

- **Ghosts:** CVF observations might be affected by the existence of 'ghosts' generated by multiple reflections between the detector and the CVF surface. Ghosts can appear away from the source image but may as well fall onto (and surround) the sky image, depending on the actual position of the source on the detector. In some cases, the photometric accuracy can be affected up to 35% by the presence of ghosts, and straylight from sources outside the theoretical field of view can affect CVF images so that sources with a flux below 10% of the background are not detectable.

- **Flat-field:** because of wheel-jitter the 'library' flat-field may not cover the same detector region as the sky image does. The effect is small in the central region of the array where the uncertainty is less than 1%. The uncertainty becomes, however, very large in the edges (up to a factor of 5 in extreme cases), where vignetting is important (for example in the case of a 6" PFOV measurement). Incomplete stabilization is another issue to consider. A large part of the small residual error in the flat-field observations is probably due to this effect. In any case, the noise levels reached are lower than expected pre-launch (1% in LW and 3% in SW).

Other error contributors like saturation, read-out, gain accuracy, dark current stability are also discussed in the 'error budget' document above refered. A summary of the main conclusions is displayed in Table 6.

Table 6: ISOCAM photometric calibration error budget.

Noise origin	magnitude	after correction
Stabilization (random)	10 x sky noise	2 x sky noise
Stabilization (systematic)	40% of source flux	15% of source flux
Saturation	$\geq$30% decrease in responsivity	
Read-out noise	LW: 0.7 ADU/g	
	SW: 2 ADU/g	
Gain	0.15% output current	
Dark current	LW: 0.5 ADU/g	0.25 ADU/g
	SW: 0.5 ADU/g	
Flat-field	LW: 0.5% (high background)	
	SW: $\leq$ 1%	
Conversion signal$\rightarrow$flux	5%	
Point Spread Function	20%	few%
CVF RSF	3%	
Ghosts	$\leq$35%	
Straylight	10% of sky flux	

Regarding flux reproducibility, repeated photometric observations on HIC 89474 throughout the whole ISO lifetime give a standard deviation of around 2% for both LW and SW detectors. Similar observations on a larger set of absolute flux calibration standards give an r.m.s. of around 5%. It was also found that the LW detector is very linear over a very large range of flux levels from a few mJy up to the saturation level. From CVF observations the derived r.m.s. is 3% for the SW part and 4% for the two LW CVF segments.

Significant improvements in the photometric accuracy of ISOCAM data can be achieved by making use of the software tools implemented in CIA, the Interactive Analysis software package for ISOCAM data reduction.

Deglitching routines are available under CIA although they only mask the frames corresponding to the glitches. Thus, a visual inspection of all pixels histories is needed for a proper masking. The impact of 'faders' and 'dippers' is related to the general problem of the transient behaviour of the CAM detectors and can be corrected using transient correction algorithms implemented in CIA, based on the so-called 'IAS method' (for LW detectors).

In general, the systematic errors introduced by incomplete stabilization can be reduced up to a 10-15% level with the IAS method and can be better than 1-2% after the application of the new transient correction routines based on the Fouks-Schubert's model in the case of CVF spectra affected by large transients inherited from previous discrete filter observations. However, the method still fails for structures with strong spatial gradients (like point sources).

Manual elimination of ghost images, which can in some cases lead to errors up to 25% in aperture photometry, is also possible with CIA, as well as the elimination of inaccuracies introduced by inaccurate flat-fields, at least in the case of rasters with sufficient background and redundancy (not possible, however, for staring observations yet).

In summary, the magnitude of all the above effects compared to pre-launch expectations are generally in good agreement. Note that in Table 6 the 5% accuracy quoted as error induced by the conversion factor from ADU/g/s to Jy is worse than the pre-launch value (2%) because the measured photometry is PSF corrected, so this error estimate includes also the uncertainty in the PSF.

The CVF Spectral Response Function (SRF) is very well constrained. Typically the accuracy is at the 3% level on average in the absence of ghosts and straylight.

4.3.3 Future plans in CAM calibration

Concerning the expected accuracies of ISOCAM's final OLP data products, this will strongly depend on whether the calibration improvements that are now available under CIA can be transfered into the OLP pipeline (we know that, certainly at least for transients, the problem of implementing the corresponding corrections in the pipeline is far from simple).

As it has previously been reported in this document, several transient correction methods have recently been implemented in CIA. The latest implemented method, the so-called Fouks-Schubert method, is claimed to reach accuracies

on the percent level. In addition, the SLICE package, intended to correct for long-term transients and applicable only to highly redundant CAM raster scans, has also represented a major improvement in the process of CAM data reaching results which are just limited by read-out and photon noise equivalent to 100-200 μJy.

However, in both cases, the determination of the effect of transients usually need a lot of interactivity during the data reduction process, which does not allow their inclusion in the CAM pipeline.

An additional problem comes from the fact that the Fouks-Schubert transient correction method is best suited for extended emission but fails for structures with strong spatial gradients (like point sources). Efforts are on-going trying to find a way in which this transient correction could also be applied to point sources, which should be first implemented in CIA, and eventually in the pipeline.

Several de-glitching methods under test could also improve significantly the calibration accuracy of CAM maps and improve point/extended source detection, as well as a better PSF fitting, which may affect the photometry substantially. This is, of course, closely related with the presence of ghosts. This is another field where progress is expected in the near future if finally a correction matrix becomes available. Again, the problem basically resides in how to make all these tools available in the CAM pipeline.

Other areas where improvements are expected in future versions of the pipeline are: astrometric correction, flat-field corrections taking the lens-wheel jitter into account, treatment of flat/dark observations and mosaic generation.

4.4 LWS

4.4.1 Improvements in OLPv8.7 for LWS

The release of OLPv8.7 (LWS upgrade), initially planned for November 1999 has been postponed to December 20, 1999.

Note that this means that when LWS data is retrieved from the ISO Data Archive and the *'Latest Processing'* button is selected the user will get the data still processed with OLPv7 until the new version is released.

A few changes are expected in version 8.7 of the LWS pipeline. Perhaps the most important one is that new data products will be derived using the new Uranus model in the LWS calibration files.

In addition, the OLPv8.7 LWS Fabry-Pérot (FP) products from AOTs LWS03 and LWS04 should show a marked improvement in the flux calibration in comparison to their OLP v7 counterparts. In OLP v7 the FP LSAN file gave the flux per spectral resolution element (in units of W cm^{-2}). In OLP v8.7 the units will be W cm^{-2} μm^{-1}, where the throughput correction (i.e. the FP transmission multiplied by the FP resolution element) has been performed using Mars as the calibrator.

The other noteworthy change in OLP v8.7 is that fixed dark currents are subtracted for all FP observations, rather than those measured during the ob-

Table 7: Flux calibration accuracy of LWS OLPv7 data products per AOT

		LWS01 Grating	LWS02 Grating	LWS03 Fabry-Pérot	LWS04 Fabry-Pérot
Point sources	Bright	30%	30%	Unvalidated	n.a.
	Medium	10%	10%	Unvalidated	n.a.
	Faint	50%	50%	Unvalidated	n.a.
Extended sources	Bright	50%	50%	Unvalidated	n.a.
	Medium	30%	30%	Unvalidated	n.a.
	Faint	50%	50%	Unvalidated	n.a.

servations themselves. These fixed set of detector dark currents originate from a series of dedicated measurements made in revolution 650.

Other minor changes are just oriented to ensure that LWS data will be Y2K compliant.

The calibration accuracy status of the instrument and the corresponding error budget have not significantly changed since the previous Status Report.

4.4.2 Current calibration accuracies and 'Error Budget' for LWS

A document describing the *LWS Calibration Status* as of November 1998 is available at:

`http://www.iso.vilspa.esa.es/users/expl_lib/LWS/LWS_Cal_Accuracy.html`

Although this report is based on OLPv7 data products, most of its content is still valid for OLP v8.7 data.

A summary of the main accuracy numbers is displayed in Table 7 as a function of the AOT and the brightness of the source observed. Note that the concept of 'bright', 'medium' and 'faint source depends on the observing mode. For the grating modes a 'bright' source means typically more than 1000 Jy at 120μm, while 'faint' could be a source with a flux density in the order of 10−50 Jy at 120μm. For the fabry-Pérot modes these numbers have to be multiplied by a factor of 10 at least.

Fabry-Pérot AOTs are not yet validated owing to a problem of misalignment of the underlying grating response profile. This is caused by uncertainty in the grating wavelength calibration. It is expected that

Some of the known sources of error affecting LWS are:

Relative Spectral Response Function: detailed examination of the shape of the continuum of Mars and other Solar System objects indicates that the Uranus model used as primary standard shows a discrepancy at the shortest wavelengths ($43 - 55$ μm) at the level of no more than 7% at the extremes of the SW1 band and this is still being investigated.

Dark current subtraction and memory effects: this especially affects spectra of faint sources. There is evidence that observation of a bright source

before a faint one caused the dark current to be higher than expected and to be decaying during the subsequent observation. In addition, dark current variations have been observed within Fabry-Pérot measurements which are presently not fully understood.

Fringes: channel fringing is seen on the measured spectra of extended or off-axis point sources. Extensive modelling of the response of the instrument has been carried out using the ASAP optical design software showing that the fringes are produced by the interference between the reflecting surface of the LWS field mirror and its support structure as the diffraction pattern of the source falls off the edge of the field mirror itself. A quantitative model, however, is not yet available that would allow the removal of the fringes given knowledge of the spatial structure of the source. Instead, a method has been developed which performs a fit for the period, amplitude and phase of the sinusoid and removes it from the spectrum by division or subtraction.

Beam profile: the pipeline processing of LWS data makes no attempt to correct for the beam shape of the instrument. Attempts have been made to determine the spatial response of LWS using spectra of Mars located at different positions with respect to the axis of the LWS as a function of wavelength. The FWHM of the esentially gaussian beam profiles obtained are $\sim$20% narrower than expected. In addition, the beam is assymetric and fringes are also present. It is expected that the situation will improve soon, now that a model for at least the core of the beam profile has been obtained (see *Beam Profile WG* section).

Non-linearity effects: Bright sources cause some of the detectors to become non-linear. The problem is complicated by photon curing of the detectors; this, in turn, causes the responsitivity of the detectors to change. An empirical method has been developed and implemented in the pipeline for the derivation of the photocurrent, and hence flux, from the voltage ramps which fits a first or second order polynomial automatically with no *a priori* assumptions about how the detectors respond, reducing the noise in the output spectra.

Time constants: The time constants of the detectors cause the shape of the spectrum (both lines and continuum) to be distorted under certain illumination conditions.

Poor order sorting: Spectra below 50 μm and between 83 and 90 μm might suffer from contamination owing to poor order sorting. An instrument model is required that will allow the determination and removal of the contamination.

The calibration accuracy of products manually processed with LIA does not strongly improve for the grating observing modes LWS01 and LWS02 for well-behaved data sets. The only changes expected concern LWS03 and LWS04 as can be seen in Table 8 below. For bright sources observed with these AOTs there is an excess component in the signal that is most likely due to straylight.

A discussion on the individual contribution to the LWS photometry 'error budget' coming from the different steps involved in LWS data processing is contained in the document: *In-orbit performance of the ISO Long Wavelength Spectrometer* by Bruce Swinyard et al. (October 1998), available at:

`http://www.iso.vilspa.esa.es/users/expl_lib/LWS/HAWAII.PS`

Table 8: Flux calibration accuracy of LWS LIA data products per AOT

		LWS01 Grating	LWS02 Grating	LWS03 Fabry-Pérot	LWS04 Fabry-Pérot
Point sources	Bright	30%	30%	50%	50%
	Medium	10%	10%	30%	30%
	Faint	50%	50%	50%	50%
Extended sources	Bright	50%	50%	50%	50%
	Medium	30%	30%	30%	30%
	Faint	50%	50%	50%	50%

Assuming a mean uncertainty in the Uranus model of ∼5% and a statistical error on the RSRF better than 0.01, for observations where the dark current is not a significant contribution to the signal, the uncertainty contributed to the measurement by the calibration process is estimated to be of the order of 7% for most detectors. In the case of faint sources, when the dark current becomes significant, the uncertainty in the measurement of the dark current begins to dominate.

Long term monitoring has shown that the repeatability of the flux calibration is within 10% for all objects not influenced by the uncertainty in the dark current measurement.

For LWS the goals originally set before the mission (an accuracy of 30% or better in the grating mode and 50% in the Fabry-Pérot mode) have in most cases been achieved for well-behaved data sets. In some areas, however, problems remain and they are the subject of further investigation.

4.4.3 Future plans in LWS calibration

The flux calibration accuracy of LWS is expected to improve significantly during the remaining post-operational phase.

The discrepancy in the shape of the Uranus spectrum is expected to be fully characterized soon. If and when confirmed, an improvement of the continuum determination at short wavelengths should be expected.

Other expected improvements in LWS calibration are the new glitch detection algorithms that will soon be available within ISAP and LIA, or the corrections for memory effects, still under investigation (see *Transients WG* section). Once a correction for memory effects will be available new RSRFs will be derived and inserted in the pipeline.

It is also expected that the availability soon of a beam profile model for LWS will significantly improve the calibration of extended sources. Interpolated beam maps, as a function of wavelength for each detector should be available on a short time scale. The absolute accuracy that will be achievable in these maps is difficult to estimate at present but the aim is to have an accuracy not worse than 10% at 1% of the beam profile. Estimating the systematic error on the flux calibration of a source of arbitrary distribution within the beam at any

wavelength is problematic as it is likely to be a function of wavelength due to the more precise sampling of fringes at longer wavelengths.

The characterization of the behaviour of the detector dark current following observations of bright sources is also expected to improve. This may lead to an improvement in the systematic error in the flux determination for some faint sources.

Detailed studies of the response of the detectors to strong sources are on going and more sophisticated methods of dealing with the problem are being investigated. It is to be expected that this problem will be solved for the final OLP v10.0.

Unfortunately, it is still not clear whether a version 9 of the LWS pipeline will exist (it should be released by mid 2000). If not, the improvements above listed will have to wait until the final OLP v10.0 (February 2001).